


REVIEW

Open Access

Cenozoic history of the Australian Monsoon



Stephen J. Gallagher^{1*} , Vera A. Korasidis¹, Gerald Auer², David De Vleeschouwer³, Jeroen Groeneveld⁴ and Beth Christensen⁵

Abstract

The Australian monsoon is part of the global monsoon and often included as a component of the Asian Monsoon system although they operate out of phase. Due to their hemispheric positions, the dry (wet) Australian winter (summer) monsoon coincides with the wet summer Asian monsoon and vice versa. The Australian monsoon controls rainfall distribution in northern tropical Australia where over 80% of the median annual rainfall occurs from December to March, the summer wet season. Three types of the Australian monsoon are distinguished based on distinct atmospheric circulation and heating patterns: a northwest *Pseudo-Monsoon*, a northeast *Quasi-Monsoon* and an *Australian Monsoon* (sensu stricto) north of Australia. While the modern climatology of the Australian monsoon has been extensively documented, its paleohistory is poorly constrained, especially in Australia's continental interior where harsh arid climatic conditions have degraded almost all physical evidence of monsoonal activity. However, reassessment of northern and central Australian terrestrial and marine sequences reveals a fairly robust Cenozoic history of this monsoon, especially for the Neogene, which we synthesize for the first time here. Evidence for a Paleogene Australian paleomonsoon is equivocal due to the small number of sites, their limited age control, and the poor preservation of flora with ambiguous affinities. Modeling and tectonic evidence suggest the northern part of the Australian Plate migrated to the (sub)tropical region (north of 30°S) creating "modern" boundary conditions for monsoonal onset by ~10 Ma. Cores off northwest Australia reveal arid late Miocene and humid Pliocene conditions were followed by the Pseudo-Monsoon at ~3.5 Ma when northern hemisphere glacial expansion "forced" the ITCZ (Inter Tropical Convergent Zone) south. Subsequently, variable humid and arid periods typify Quaternary high-amplitude glacio-eustatic cycles until ~1 Ma, when arid conditions expanded across Australia. Glacial/interglacial cyclicity and obliquity/precession insolation during terminations modulated *Pseudo-Monsoon* intensity when the ITCZ migrated northward (during glacial) and southward (during interglacial periods) from ~1 Ma to present. From ~1.6 to 1 Ma, precession paced *Pseudo-Monsoon* variability. Mega-lake expansion in central Australia and fluvial intensification generally correspond to wetter interglacial periods. Lake Eyre monsoonal shorelines may have been influenced by abrupt millennial events. Monsoonal conditions re-established near the base of Holocene as the ITCZ migrated across northern Australia. The *Australian Monsoon* (sensu stricto) and *Quasi-Monsoon* (a) initiated from 12.5 to 11 ka; (b) intensifying from 9 to 2 ka; then (c) weakened, possibly due to the onset of ENSO intensification. The *Pseudo-Monsoon* was established at ~14.5 ka off northwest Australia intensifying from 11.5 to 7 ka. It weakened after ~7 ka north of 15°S and ~5 ka to the south. In the absence of a topographic influence, insolation (precession/obliquity), abrupt millennial events and/or ITCZ variability across northern Australia were important controls on Quaternary Australian monsoon intensity. Further investigations of deeper time pre-Quaternary records off northwest and northeast Australia will reveal the paleohistory of this important domain of the Global Monsoon.

Keywords Paleomonsoon, Pseudo-Monsoon, Quasi-Monsoon, Cenozoic, Quaternary, Proxies

*Correspondence:
Stephen J. Gallagher
sjgall@unimelb.edu.au
Full list of author information is available at the end of the article

1 Introduction

The Australian monsoon is a domain of the global monsoon that is often included as part of the Asian monsoon (Wang et al. 2017; Clift et al. 2022). However, due to their opposing hemispheric positions, the dry (wet) Australian winter (summer) monsoon coincides with the wet (dry) summer (winter) Asian Monsoon (Beaufort et al. 2010). The Australian monsoon controls rainfall distribution in the northern tropical region (400,000 km²) of Australia (Suppiah 1992; Sturman and Tapper 1996) where over 80% of the mean annual rainfall (> 350 mm– > 1200 mm) occurs from December to March, the summer wet season (Fig. 1c). The temperature gradient between the northern Australia landmass and the surrounding oceans during the austral summer produces moist northwesterly wind from the Indian Ocean, replacing the more arid austral winter easterly trade winds during the dry season (Wang and Zhang 2017). Strong austral summer heating of northern Australia also reduces atmospheric pressure cutting off the trade winds with northwesterly and westerly winds (Gentilli 1971). The region north of 25°S in Australia is generally subject to summer wet and winter dry climates comparable to the tropical monsoonal climate of Africa and Asia (Suppiah 1992; Clift et al. 2022). However, there is enough variation in the controlling atmospheric conditions to distinguish three distinct types of monsoonal regions.

Australian monsoon classification: Three types of monsoons are identified based on a meteorological definition, i.e., having distinct heating processes and atmospheric circulation patterns across northern Australia (Gentilli 1971, 1995; Suppiah 1992, 1995). The **Australian Monsoon** (denoted as *sensu stricto* in this review to distinguish it from the generalized descriptions of the Australian monsoon) exhibits a classic monsoon structure and reaches an atmospheric convection height of 3000 m thick in the region between 130°E and 145°E (Fig. 1a, c), north of 18°S. This constitutes a “true” monsoon flow as it is derived from austral summer cross-equatorial flow and equatorial westerlies from maritime airmasses at 850 hPa (Gentilli 1971, 1995; Suppiah 1992). This is in contrast to the westerly monsoonal flow toward and over the Kimberley region west of 124°E in

northwest Australia (Fig. 1a, c). This westerly flow is shallower, weaker and more localized and is not considered to be a true monsoon by Gentilli (1971, 1995). Instead, Gentilli (1971, 1995) considers the southwest trade winds deflected by a semi-permanent heat low near Pilbara to be a “**Pseudo-Monsoon**” (Fig. 1a, c), since this monsoonal flow has not crossed the equatorial region and is made up of drier anti-cyclonic air recycled from the ocean northwest of Australia. Similarly, this author suggests a “**Quasi-Monsoon**” exists East of 145°E where flow is deflected southeastward due to a heat low region in western Queensland (Fig. 1a, c) with most of its moisture derived from winds from the Pacific (Suppiah 1992; Kershaw and van der Kaars 2012).

The classification above is confirmed by the presence of three distinct and persistent monsoonal troughs in global monsoonal 850 hPa geopotential height Pentad (5 day, 1979–2007) datasets analyzed by Wei-Hong and Shuai-Qi (2010) supporting Gentilli’s original threefold subdivision.

Thus, we recognize and structure our review of the Australian paleomonsoon around these three types of monsoon and their spatial distribution (Fig. 1): the **Australian Monsoon** (*sensu stricto*) in northern Australia, the **Pseudo-Monsoon** (northwest Australia) and the **Quasi-Monsoon** (northeast Australia). Below, we describe the climatological impacts of the modern monsoon in advance of a description of the paleoclimatological history.

The presence of zero mean zonal winds at low levels at the boundary between the easterly trade winds and the equatorial westerlies is known as the “monsoon shear line” or monsoonal trough (Figs. 1a, c, 2a, c) (McBride and Keenan 1982; McBride 1987; Suppiah 1992; Zhang and Moise 2016). This feature occurs daily in the austral summer across the area from 105 to 165°E (McBride and Keenan 1982). It is the region where tropical cyclones form (Fig. 2a, c) from ~25 to 17°S. Westerly winds to the north of the shear line are associated with increased summer monsoonal cyclonic rainfall, whereas low rainfall south of the shear line occurs in the easterly trade wind regime (Fig. 1c, Suppiah 1992). Episodic summer tropical cyclones across northern Australia and the Arafura Sea

(See figure on next page.)

Fig. 1 **a** Location of monsoonal rivers and lakes with the mean monsoon shear line (McBride 1987), Inter Tropical Convergence Zone (ITCZ), and position of major monsoon regions (cf. Gentilli 1971, 1995; Suppiah 1992); **b** Location of additional monsoonal archives (see Table 1 for numbered site details) with desert locations and dust path (black arrows) (adapted from Blewett 2012). Base map adapted from General Bathymetric Chart of the Oceans (GEBCO) www.gebco.net and adapted from Gallagher and deMenocal (2019); **c** Generalized average atmospheric circulation for January (orange arrows) and **d** July with key locations indicated in red adapted from Gentilli (1971). The monthly CMAP precipitation climatology from Arkin and Xie (2022); **e** Modern floral distribution in Australia and Papua New Guinea (PNG; adapted from Kershaw and van der Kaars 2006); **f** Seasonal rainfall zones of Australia adapted from http://www.bom.gov.au/jsp/ncc/climate_averages/climate-classifications/index.jsp?maptype=seasgrpb#maps (accessed 30/05/2022)

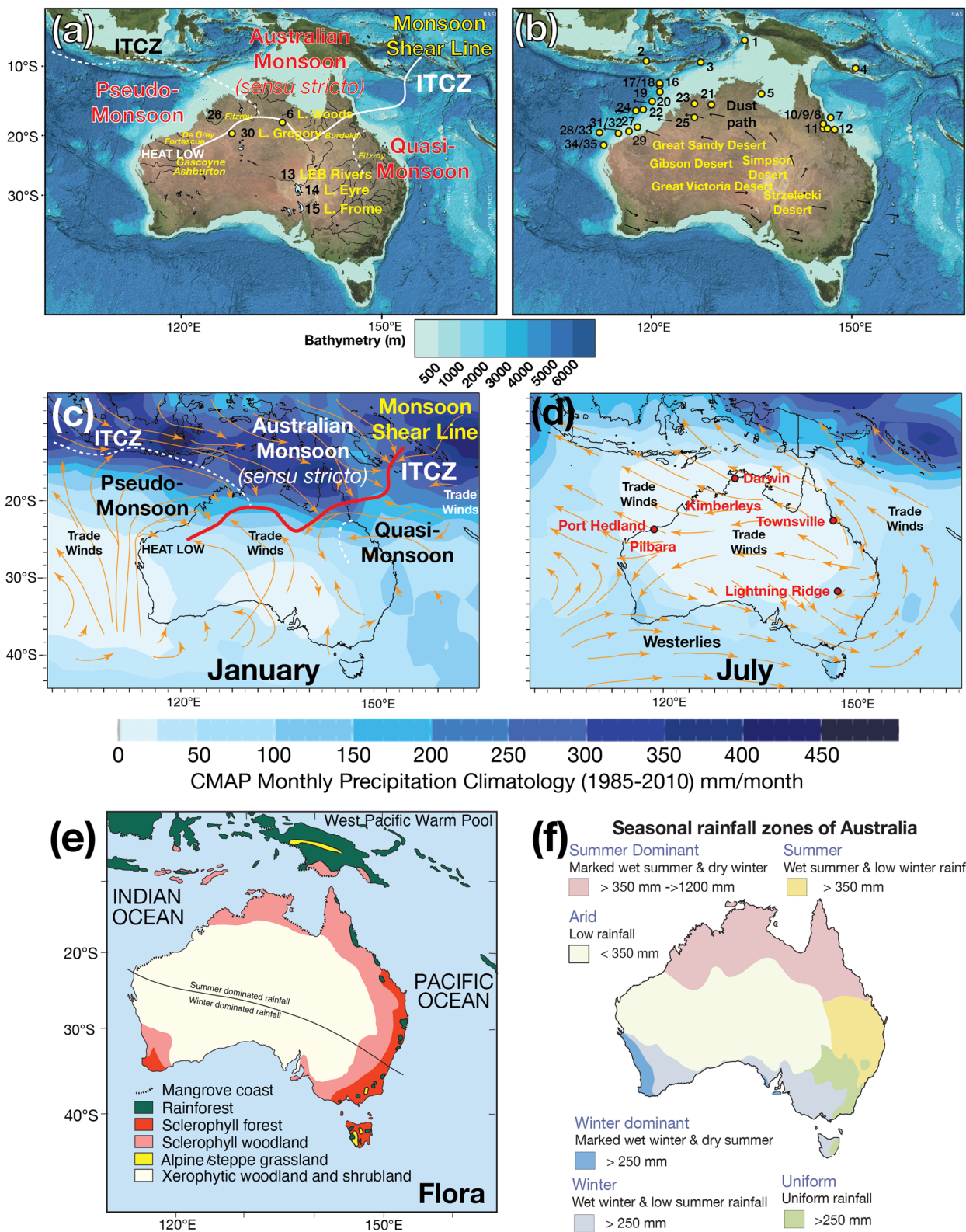


Fig. 1 (See legend on previous page.)

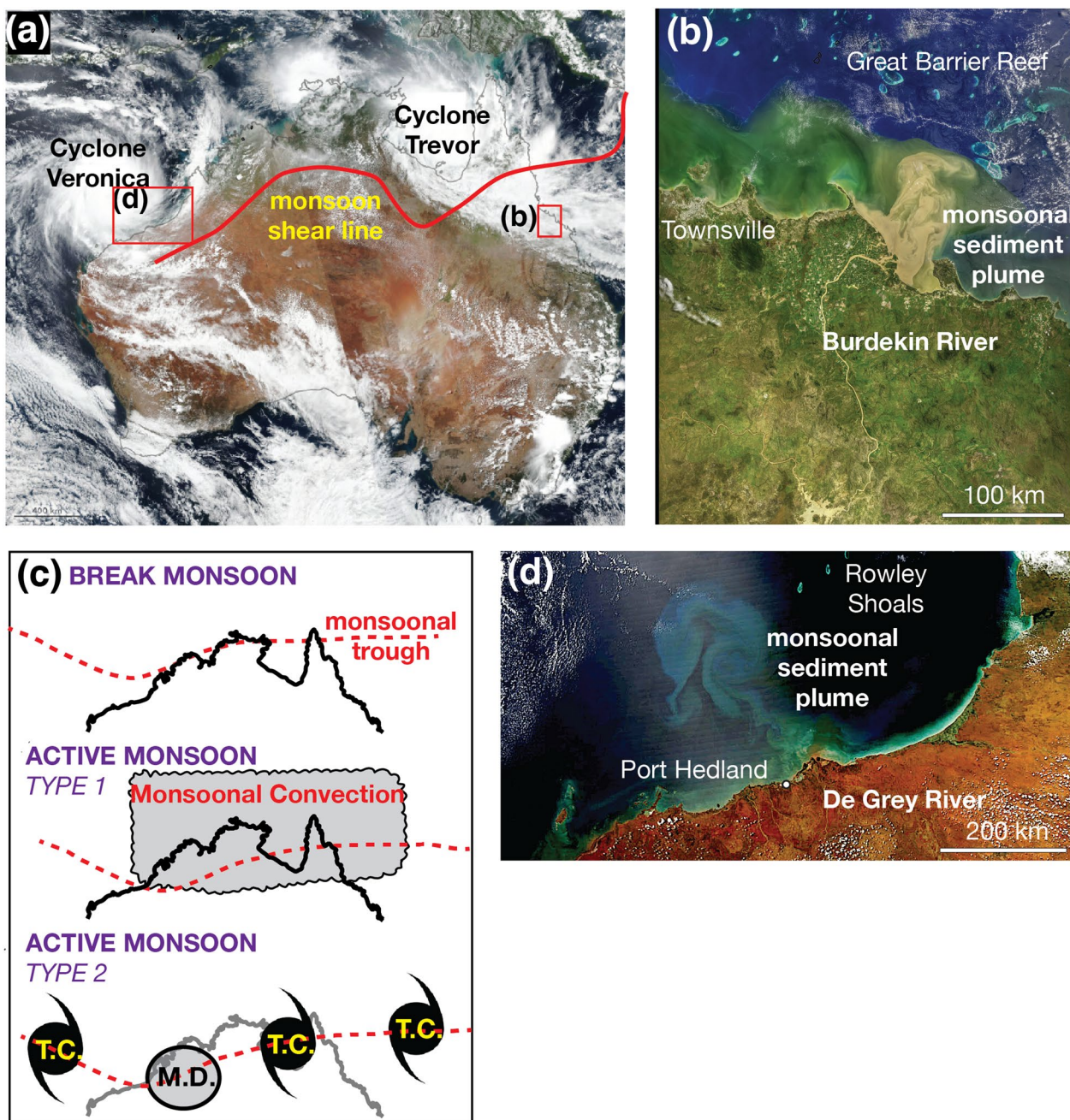


Fig. 2. **a** Location of two cyclones across northern Australia north of the monsoon shear line on March 22, 2019 (from <https://earthobservatory.nasa.gov/images/144733/northern-australia-braces-for-a-pair-of-cyclones>, accessed 30/05/2022). **b** A monsoonal sediment plume from the Burdekin River Queensland reaches the Great Barrier Reef on February 11, 2019 (from <https://oceancolor.gsfc.nasa.gov/gallery/620/>, accessed 30/05/2022). **c** Typical Australian monsoon tropical cyclogenesis (T.C. Tropical Cyclone, M.D. Monsoonal Depression) where two types of active monsoon systems may occur (either tropical cyclones or storms due to monsoonal convection and once the monsoon ceases this may be followed by a monsoonal trough (adapted from McBride 1987); **d** satellite imagery of a post-cyclonic sediment plume from the mouth of the De Grey River that reached the northwest shelf on the March 17, 2013 (from https://www.nasa.gov/mission_pages/hurricanes/news/rusty-sediment.html, accessed August 3, 2020). The position of **c** and **d** is indicated with red squares in panel (a).

from November to May deliver significant rainfall (up to 3000 mm during tropical cyclones) during the monsoon season (Fig. 2). The resulting ephemeral runoff causes

continental flooding and delivers significant plumes of fluvial siliciclastic sediment to the offshore shelf regions of northern Australia (Fig. 2b, d). Most tropical cyclones

originate between 9° and 19°S north of the 27 °C isotherm on the monsoon shear line in the southwest Pacific (Figs. 1, 2; McBride and Keenan 1982; McBride 1987; Suppiah 1992) and track westward (Sturman and Tapper 1996). Tropical cyclones may form in any tropical waters around Australia. However, key areas for cyclogenesis are Port Hedland, northwest Australia, near Townsville, Queensland and east of Darwin (Figs. 1, 2, Hobbs et al. 1998).

The equatorial trough or Intertropical Convergence Zone (ITCZ, Fig. 1c) is a wide region of convergence of tropical easterly flow from the equatorial side of the subtropical high-pressure cells in both hemispheres (Sturman and Tapper 1996). It exerts a significant control on the Australian monsoon. The ITCZ typically is located north of the equator, but it shifts southward in the eastern hemisphere due to changes in continental heating leading to peak northern Australian wet season (Williams et al. 2009). In Australasia, the ITCZ is 10 to 15° north of the equator in the austral winter. In summer, it migrates southward over northern Australia (to ~18°S), marking the southern limit of the Australian Monsoon (*sensu stricto*) (Fig. 1c). Australian paleomonsoon timing and strength are interpreted to be influenced by insolation variability due to obliquity and precessional forcing (Wyrwoll et al. 2007, 2012). The Australian summer monsoon lacks the topographic influence that controls the Indian–East Asian summer monsoon and is, therefore, weaker and more sensitive to variations in insolation (Wyrwoll et al. 2007).

While the modern climatology of the Australian monsoon has been extensively researched, knowledge of its paleoclimatology is not as well-known, especially in continental Australia. Seasonally harsh arid climatic conditions often destroy evidence of fluvial/lacustrine activity, making sediment and fossil archives difficult to date and interpret (Gallagher et al. 2017; Gallagher and deMenocal 2019). An (2000) speculated that the histories of the Australian and East Asian Monsoons might be linked and that they originated prior to 7 Ma; however, there is no clear evidence for this age estimation provided in An (2000). Bowman et al. (2010) suggested that “the (Australian) monsoon is of great antiquity” based on the high diversity and strong adaptations of biota to the wet-dry tropical climate and their enhanced general adaptability, although these authors do not provide the estimates of this inferred age. Significant progress has been made in the last two decades investigating Quaternary monsoonal influenced cave, lake shoreline, and fluvial facies in northern and central Australia (see Sect. 5) where pre-Quaternary archives are typically rare or absent. Furthermore, new sediment plume records preserved in offshore ocean coring archives off northwest and northeast Australia are

yielding well-preserved and dated Quaternary and pre-Quaternary records (see Gallagher and deMenocal 2019; Clift et al. 2022). Combined, these are beginning to reveal the deep time history of the Australian paleomonsoon.

This paper describes the various indicators and geomorphic features used to interpret the history of Australian monsoonal paleoprecipitation and rainfall seasonality. Then, we describe the long-term global climate and tectonic controls on the Australian paleomonsoon. Following this, we review over thirty-five Quaternary and pre-Quaternary offshore and continental monsoonal archives from northern and central Australia. Next, we suggest possible future perspectives and directions for Australian paleomonsoon research. Finally, we arrive at a summary of the Cenozoic history of the Australian paleomonsoon.

2 Controls on Australian paleomonsoon over the last 50 million years

The Earth has transitioned from an ice-free greenhouse to an icehouse climate over the last 50 million years (Fig. 3; Zachos et al. 2001, 2008; Westerhold et al. 2020). During this time, Australia has progressively moved northward, with its northernmost continental margin reaching 30°S by ~30 Ma (Fig. 3). Low-latitude seasonality was likely enhanced with the onset of the first glaciation (Oi at 33.8 Ma), and ocean circulation intensification due to the opening of gateways in the widening Southern Ocean (Exon et al. 2000). By 20 Ma, most of the present monsoonal influenced region of Australia was north of 30°S (Fig. 3d). As Australia traveled further northward, seasonality was further enhanced due to the uplift of the Tibetan Plateau from 15 to 5 Ma (Zhisheng et al. 2001; Thomson et al. 2021), establishing a strong equator to south polar temperature gradient (Bowman et al. 2010) associated with the strengthening of the Indian summer monsoon (Clift et al. 2022). Indonesian Gateway restriction and uplift and exposure of the Isthmus of Panama by ~3 Ma led to similar modern-day oceanic and atmospheric circulation patterns in the Pacific (O’Dea et al. 2016; Gallagher et al. 2024). Thus by 3 Ma and possibly even as far back in time as 15 Ma, conditions were suitable for the “modern” monsoon across northern Australia (Bowman et al. 2010). The transition from the 41 kyr world of the Pliocene to the 100 kyr climate oscillations of the middle Pleistocene transition (1.2 to 0.8 Ma) was accompanied by glacial/interglacial cycles causing marked monsoonal rainfall variability (Bowman et al. 2010; Gallagher et al. 2014). Over the last 2 Ma, interglacial wetter (stronger monsoon) and drier glacial (weaker monsoon) conditions prevailed in Australia’s northwest (Gallagher et al. 2014; Gallagher and Wagstaff 2021). Arid conditions in central and southern Australia intensified

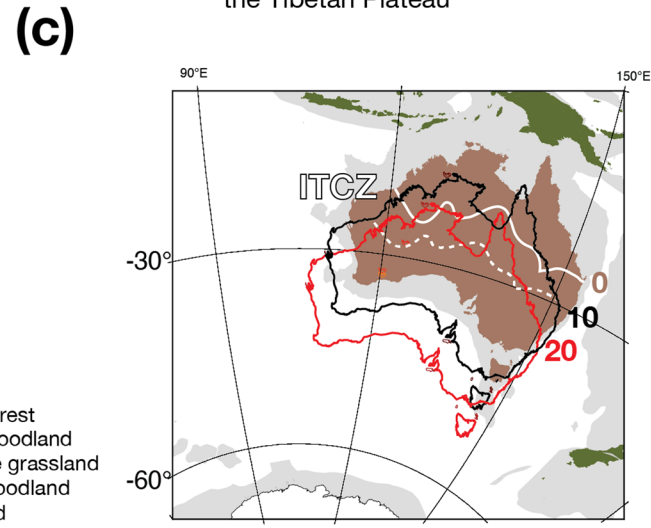
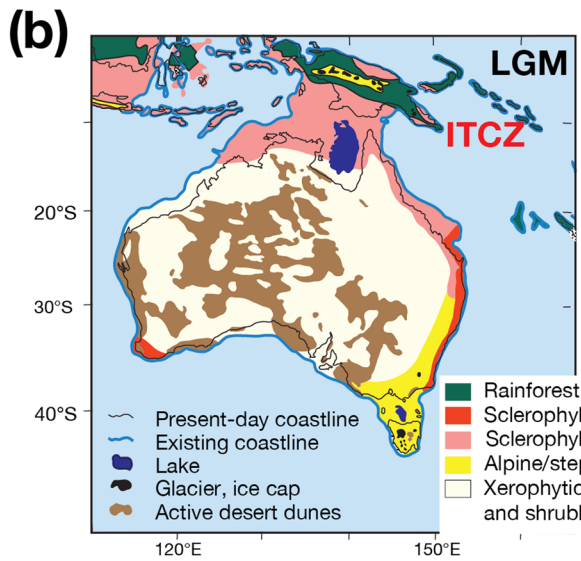
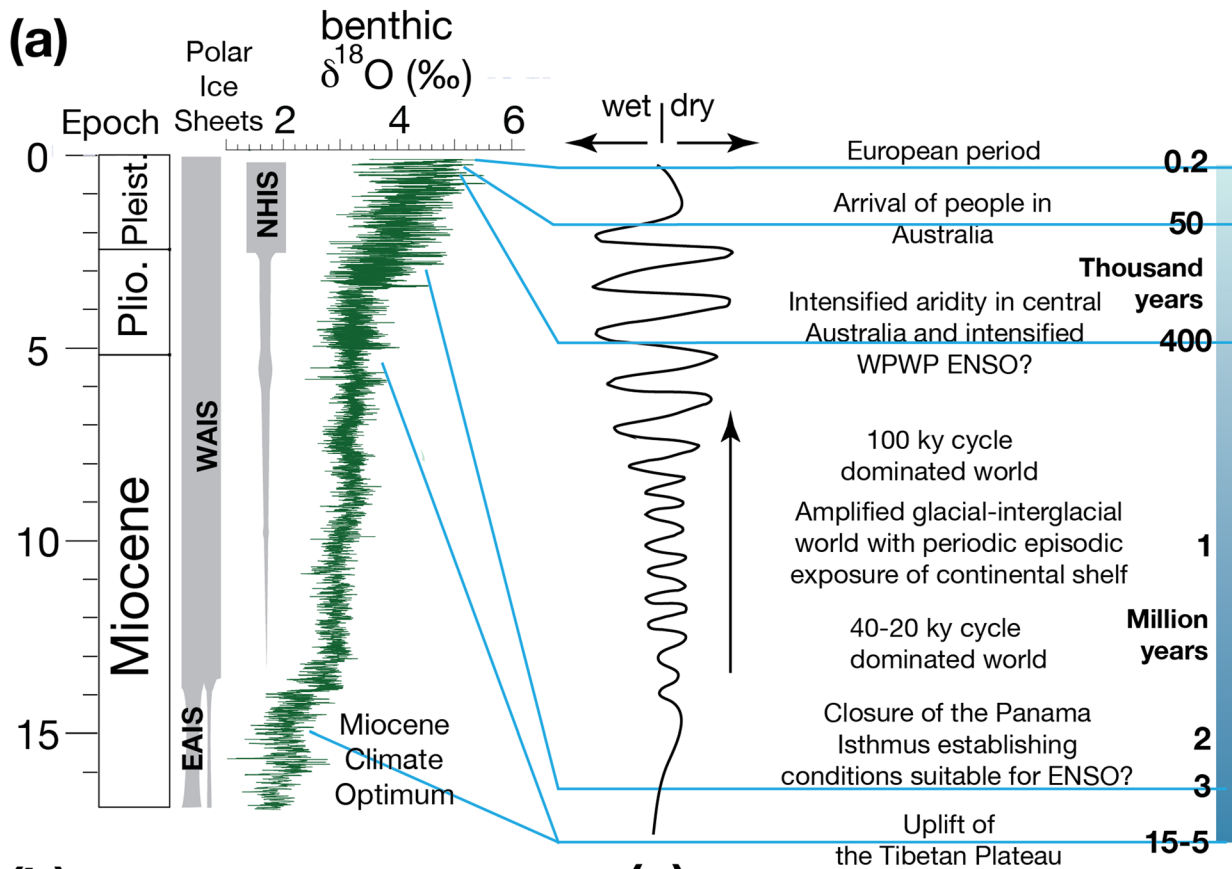


Fig. 3 A summary of the setting of the Australian paleomonsoon: **a** Cenozoic Global Reference benthic foraminiferal Carbon and Oxygen Isotope Dataset (CENOGRID) from ocean drilling core sites spanning the past 17 million years (adapted from Westerhold et al. 2020); with a summary of the tectonic and climate controls on the Australian monsoon (adapted from Bowman et al. 2010). WAIS = West Antarctic Icesheet, EAIS = East Antarctic Icesheet, NHIS = Northern Hemisphere Icesheet. **b** The LGM (Last Glacial Maximum) palynoflora and paleogeography of Australia and PNG (adapted from Kershaw and van der Kaars 2006); **c** Plate tectonic motion of Australia since 20 Ma, with the modern average position of the ITCZ and that inferred at 10 Ma (dotted line) adapted from Gallagher and deMenocal (2019).

in a stepwise manner, with drying after ~1.5 Ma and 0.6 Ma, with the disappearance of megalakes in south-east Australia at ~1.5 Ma (McLaren et al. 2014) and the expansion of the monsoon-influenced Simpson Desert (Fig. 1b) around 1 Ma (Fujioka and Chappell 2010).

Palynofloral records from the Last Glacial Maximum (LGM; Figs. 1, 3) suggest enhanced arid conditions with xenophytic woodland and shrubland dominating the Australian continent, while sclerophyll woodland and rainforests were displaced toward the equator (Kershaw and van der Kaars 2006; Fig. 3) suggesting limited monsoonal influence in northern Australia when the ITCZ was positioned close to the equator (Williams et al. 2009). In the Banda Sea and northwest Australia, paleoceanographic records indicate monsoon resumption after ~14 ka after being less intense for the previous 60 ka when the ITCZ lay north of the Banda Sea (Spooner et al. 2005; Wyrwoll and Miller 2001).

3 Interpreting paleoprecipitation

In this section, we describe geomorphic and marine evidence used to interpret paleoprecipitation in the pre-instrumental paleoclimate record of the Australian paleomonsoon (see Mann 2002 and Baker 2009 for extensive summaries of paleoprecipitation indicators in the geological record). However, there are fewer methods that may be used to estimate precipitation seasonality (i.e., direct seasonal monsoonal activity in summer versus winter). In our synthesis below, we find that higher precipitation estimates in monsoonal latitudes of Australia are generally attributed to increased monsoonal activity in the absence of evidence of seasonality. Various paleorainfall indicators and geomorphic features are described below, with examples of their application in an Australian context. The review of records outlined below focusses on the *positive* evidence of paleoprecipitation in the depositional record. Many of the geomorphic features and indicators for paleo-rainfall are nevertheless limited in their usefulness by the strongly erosive and harsh weathering environment of the terrestrial realm across northern and central Australia (Fitzsimmons et al. 2013). Thus, terrestrial climate archives, by their very nature, are often full of gaps and incomplete. In addition, terrestrial archives are often very difficult to date due to the presence gaps and the lack of available material to date (e.g., woody material for carbon dating, spores, pollen and other fossils). Nevertheless, as described below, much progress has been made in interpreting the monsoon record of terrestrial sequences (see review). More complete archives are present offshore from the Australian monsoonal regions, and while these may be subject to reworking and oceanic current effects that may also produce gaps, the high-resolution integrated bio-, magneto- and isotope stratigraphy

available in the marine environment enables detection of any gaps in deposition (Groeneveld et al. 2021). Significant long-term Cenozoic climate records have been constructed from cores obtained by ocean drilling of the Australian monsoon region providing a framework for evaluating older continental records (Clift et al. 2022).

3.1 Geomorphic and facies evidence of monsoonal activity

The distribution of fluvial, lacustrine, eolian, swamp, desert geomorphological features, marine facies and cave deposits is related to relative paleoprecipitation. The presence/absence, age, and spatial distribution of these features and their facies have been used to interpret the history and intensity of wetter and drier conditions in Australia, especially in the Quaternary (e.g., Nanson et al. 2008).

(i) *Fluvial deposits in ephemeral drainage systems*

Optically stimulated luminescence (OSL) and uranium series dating of quartz grains has been used to constrain the timing of fluvial deposits in the monsoon-influenced Lake Eyre basin (Nanson et al. 2008; Fig. 1). The limitations and problems associated with dating fluvial sediments using these techniques are outlined comprehensively in Nanson et al. (1991), Duller (2004), Rhodes (2011) and Kock et al. (2009). In particular, finding suitable quartz grains in sand layers is often an issue especially in high energy river facies, and OSL is limited to strata younger than 100 ka (Kock et al. 2009). Uranium series dating is used to get estimates of the time elapsed since carbonate precipitation of the sediment and provides a minimum age, and it therefore relies on the availability of carbonate in the strata for such dating, and the gap between sedimentation and precipitation may be unknown (Kock et al. 2009). Despite these limitations, the frequency of deposits has been used to determine episodes of enhanced river discharge during wetter events over the last 280 ka. Wyrwoll et al. (1992) used palynology, radiocarbon dating of organic-rich sediment and stratigraphic studies of fluvial sediments to document relative Australian monsoonal intensity in the west Australian Fitzroy River (Fig. 1) over the last 6.5 ka.

In summary, OSL and uranium series dating may be used to date river deposits in Australia's monsoon-influenced Lake Eyre basin back to 280 ka. While combined with palynology and radiocarbon dating, these techniques have been used to chart late Quaternary monsoonal intensity in the Fitzroy River in the Kimberley region.

(ii) *Lake shorelines facies in northern and central Australia*

The age of the maximum height of lake paleoshorelines related to pluvial phases in monsoonal Australia (e.g., lakes Woods, Gregory, Eyre and Frome) are interpreted

to be related to increased monsoonal rainfall activity (e.g., Fitzsimmons et al. 2013). Conversely, dating lake shoreline retreat (and related lunette formation) is used to infer the onset of more arid conditions (McLaren et al. 2014). Cohen et al. (2012, 2015) and Fu et al. (2017) used OSL (see comments on the limitations of this technique by Kock et al. 2009 and Rhodes 2011), and radiocarbon dating of freshwater molluscs to date measured paleo-shoreline heights of Lake Eyre and Lake Frome to determine their pluvial history over the last 200 ka.

In summary, the age of the maximum shoreline heights of lakes Wood, Gregory and Eyre in monsoonal Australia is interpreted to be related to maximum pluvial phases during monsoonal periods. In contrast, lake shoreline retreat and lunette formation are related to increased arid conditions. These shoreline records extend to over 200 ka.

(iii) Facies variability in marine cores

Huge plumes of cyclone-sourced river sediment are delivered across the continental shelves of northern Australia during the summer wet season (Fig. 2b, c). Conversely, relatively minor terrestrial sediment arrives onto these shelves during the dry season (Gallagher and deMenocal 2019). Offshore northwest Australia, the Quaternary sedimentary record in sedimentary cores reveals that periods of increased terrigenous influx (clay-rich facies) alternate with carbonate-rich (non-skeletal (oolitic) and skeletal limestones) that are interpreted to represent periods of increased monsoonal activity alternating with periods of drier more arid conditions over the last million years (Gallagher et al. 2014, 2018; Stuut et al. 2014, 2019; Gallagher and deMenocal 2019; Gallagher and Wagstaff 2021). Although sea level oscillations related to glacial-interglacial variability have a clear impact on facies changes, regional subsidence was nevertheless sufficient to preserve the characteristic facies related to long-term monsoonal/aridity variations (Gallagher et al. 2014, 2018; Gurnis et al. 2020).

In summary, during dry seasons, minimal terrestrial sediment reaches shelfal regions of offshore Northwest Australia, while in the summer wet season, cyclone-driven fluvial sediments create plumes across the continental shelf regions. In cores, this is represented by alternations of siliciclastic and carbonate facies that have been influenced by glacial/interglacial climate variability over the last 2 million years.

(iv) Dust content in offshore cores

In the dry season, northwesterly trade winds transport dust (the dust path in Fig. 1b) across the continent, depositing it in the offshore archives of northwest Australia (Stuut et al. 2014). Paleodust archives have been analyzed in onshore and offshore Australian successions using particle size analyses and trace element ratios (such

as Nb/Ta, Zr/Hf and Y/Ho) to determine the relative intensity of drier more arid conditions during the Quaternary (see summaries of the techniques used to analyze dust flux and their limitations in Hesse and McTainsh 2003; Stuut et al. 2014; De Deckker 2019).

(v) Sand dunes and desert pavements in central Australia

A combination of sedimentology, geomorphology, and stratigraphy (carbon, cosmogenic, and OSL dating) has been used to map and determine the age of arid zone features such as sand dune and desert pavement formation in Australia's arid interior (see Hesse 2016; Fitzsimmons et al. 2013; Fujioka and Chappell 2010 for comprehensive reviews on the limitations and potential for dating sand dunes and desert pavements). For example, the expansion of the Simpson Desert sand dune field at ~1 Ma related to increasing aridification of Australia was estimated using a combination OSL and cosmogenic dating of dune sediments and pavements (Fujioka et al. 2009).

(vi) Caves and speleothems in northern Australia and the Indonesian archipelago

Chronologically well-constrained carbon/oxygen isotope and trace elemental analyses of speleothems are routinely carried out to document global monsoon variability (see McDermott 2004; Fairchild and Treble 2009; Wong and Breecker 2015 for comprehensive summaries of the precision and limitations of speleothem trace element and stable isotope analyses). Compared to northern hemisphere regions, monsoon zone speleothem studies are not particularly common in Australia. Denniston et al. (2013a, b, 2017) carried out stable isotope analyses on late Quaternary speleothem in the Kimberley region (Fig. 1) of northwest Australia to document up to 40 ka of monsoonal history. Other monsoonal speleothem studies are from the Australian Monsoon (*sensu stricto*) region near the equator in the Indonesian archipelago where evidence of Quaternary monsoonal variability is preserved in stalagmite stable isotope and trace elemental records (Griffiths et al. 2009; 2010; Krause et al. 2019). In particular, the coherence between the trace elemental ratios (Sr/Ca and Mg/Ca) with stable isotope values in stalagmite speleothems in Liang Luar Cave in Flores Island (Loc. 2, Fig. 1) is interpreted to be due to changes in the hydrology above the cave system due to Holocene Australian monsoon variability (Griffiths et al. 2010).

In summary, well-dated stable isotope and trace elemental records of speleothems are commonly used to research global monsoon variability. However, these types of studies are not as common as Northern Hemisphere studies. Limited studies include a record as old as 40,000 years in the Kimberley region. A record near the equator in Flores Island reveals Holocene Australian monsoon variability.

3.2 Marine and terrestrial fossil evidence for paleoprecipitation

Terrestrial and marine fossils provide valuable insight into Australia's paleoprecipitation record. To reconstruct paleoprecipitation from fossil floral records (i.e., palynoflora or macroflora), leaf-morphology-based approaches which involve inferring paleotemperature and other climatic parameters from the physiognomy of fossil leaves, and the nearest living relative (NLR) approach (Harris et al. 2014) may be used, this uses a taxonomic approach to derive climate parameters from fossil pollen assemblages based on the climatic ranges of their present-day nearest living relatives (Dodson and Macphail 2004; Ker-shaw et al. 2007).

A strength of the leaf-morphology-based approach is that it provides quantitative estimates that do not depend on assigning fossil leaf forms to modern taxa and their current climate affiliations (Uhl et al. 2003). However, assumptions made when applying leaf-morphology-based paleoclimate methods (i.e., calibrations between leaf morphology and climate parameters are stable through time and that fossil leaf collections are sufficiently representative of the source vegetation) are limitations of this approach (Hollis et al. 2019). A strength of the NLR approach is that it uses the presence or absence of individual taxa in fossil assemblage, rather than relative abundance, thereby reducing taphonomic biases (Pross et al. 2000; Utescher et al. 2014). A weakness of this approach includes the assumption of uniformitarianism (i.e., that the climate tolerances of modern species can be extended into the past). In addition, a range of factors such as biogeographic history and competition also influence the modern distribution of a plant species (Hollis et al. 2019). A multiproxy approach to reconstruction of land-based precipitation parameters is therefore advocated where possible, including alternative leaf-morphology-based methods and taxonomic (nearest living relative) approaches.

Other useful fossil archives include charcoal (Haberle 2005; Field et al. 2017) and plant wax n-alkane distributions (Andrae et al. 2018). Beaufort et al. (2010) used nanoplankton assemblage data to document paleoproductivity variability related to Australian monsoon dynamics over the last 150 ka. Similarly, Holbourn et al. (2005) used benthic foraminiferal assemblages to document paleoproductivity variations due to monsoonal variability over the last 460 ka in the Banda Sea.

3.3 Geochemical evidence of paleoprecipitation

(i) X-ray fluorescence of sedimentary cores

X-ray fluorescence (XRF) core scanning-derived data has recently become a useful to determine the history of both dust flux/aridity as well as riverine influx, and thus

precipitation variability offshore Australia from the Neogene to Holocene (e.g., Kuhnt et al. 2015; Ishiwa et al. 2019; Stuu et al. 2019; Auer et al. 2020). The principle of using XRF-derived data is to use relative elemental abundance as climatic indices (see comprehensive summaries on the usefulness, precision, limitations and future potential of sediment XRF data analyses in Rothwell and Croudace 2015a, 2015b). For instance, in modern dust, iron, titanium, and zirconium are primarily concentrated within heavy minerals, a common component of eolian dust (Stuu et al. 2014). Relative potassium (K) and aluminum (Al) abundance is more prominently associated with clay minerals, which tend to be a dominant component of riverine influx (cf. Kuhnt et al. 2015). Elemental ratios are often “normalized” to calcium (Ca), as it is commonly also associated with biogenic carbonate production in marine environments, allowing for a correction of possibly variable dilution of dust and riverine influx by changing local biogenic carbonate accumulation (see Stuu et al. 2014; Kuhnt et al. 2015). Recent studies along the West Australian Shelf use these XRF data to emphasize the high congruence of Australian climatic records along a latitudinal transect (Stuu et al. 2019; Auer et al. 2019, 2020; De Vleeschouwer et al. 2019, 2022), and illustrate the importance of strong age control (Auer et al. 2020). The results of these studies highlight a progressive and latitudinally concurrent switch from riverine influx-dominated to dust flux-dominated regimes during the late Pliocene and the subsequent establishment of more seasonal monsoonal climatic patterns during the Plio-Pleistocene following the initiation of northern hemisphere glaciation around 3.0 Ma (Fig. 3; Raymo 1994; Westerhold et al. 2020; McClymont et al. 2023).

In summary, X-ray fluorescence (XRF) core data is a valuable tool for reconstructing Australian monsoonal climate variability. It has mainly been applied to cores off Northwest Australia, where it has been used to estimate relative dust flux related to aridity and fluvial input from monsoonal plumes of sediments that reach shelfal regions.

(ii) Downhole wireline log data variability in offshore cores

Downhole logs and outcrop natural gamma radiation (NGR) data are powerful datasets often used in paleoclimate analyses and cyclostratigraphy (see Peng et al. 2024 for a review on the advantages, disadvantages and future potential for interpreting these types of data). Downhole wireline logging gamma data or core-derived total natural gamma radiation (NGR) spectral measurements can be decomposed into its contribution from K, U and Th decay (see reviews in de Vleeschouwer et al. 2017 and Peng et al. 2024). These three elements provide

geochemical information on sedimentary composition, which in turn can be used as an indicator for dust flux and continental riverine influx, and by extension relative changes in precipitation variability of the hinterland.

For example, the abundance of K in the sediment is directly related to potassium-bearing minerals, chiefly smectite/illite and K-feldspar, which are commonly associated with the riverine influx into marine environments (Christensen et al. 2017; Groeneveld et al. 2017).

The ratio between K and Th can be used as a first-order indicator for clay-mineralogy, with high values related to kaolinite and chlorite. Along the north Australian margin, kaolinite has been used as an indicator for humid and warm climate conditions (Gingele et al. 2001). By contrast, when analyzing marine archives within the northwest Australian dust path, one needs to consider the unusual kaolinitic profiles in the Australian regolith (Thiry et al. 2000, 2006). Eolian-transported kaolinite in this setting is thus interpreted as an indicator of arid conditions, rather than as the classical interpretation as a proxy for humid/warm climatic conditions (Fagel 2007). In the Australian dust path (Fig. 1b), U and Th are again primarily related to heavy minerals associated with continental dust flux (Christensen et al. 2017; Groeneveld et al. 2017), with both elements representing radiogenic components of zircon and rutile, for instance. The abundance of surface and near-surface uranium deposits in Northwest Australia (Geoscience Australia 2015) provides additional support for linking U and dust fluxes (Christensen et al. 2017). While uranium can also be related to the organic matter in specific carbonate-dominated sedimentary environments (see Auer et al. 2016, 2021), a strong co-variation of both U and Th in marine archives can generally be considered indicative of variability in dust/riverine flux (Hesselbo 1996; Hladil et al. 2006; Christensen et al. 2017). The application of various NGR records provided both long-term and orbital trends of monsoonal variability and precipitation along the western shelf of Australia over the Neogene and Quaternary (Christensen et al. 2017; Groeneveld et al. 2017; De Vleeschouwer et al. 2018).

In summary, natural gamma radiation (NGR) data from downhole logs are very useful for paleoclimate and cyclostratigraphic studies of offshore Australian monsoonal strata. The relative abundance of potassium, uranium and thorium may be related to dust flux and riverine influx and precipitation variability from the Neogene to Quaternary.

3.4 (iii) *G. ruber* Nd/Ca of foraminifera in marine cores

Although ϵNd values of planktic foraminifera typically reflect bottom water variability (Tachikawa et al. 2014), Liu et al. (2015) used neodymium over calcium (Nd/Ca)

ratios (REE or Rare Earth Element/Ca) in the shells of the planktic foraminifera *Globigerinoides ruber* to interpret precipitation-related river runoff off the coast of equatorial Papua New Guinea. This follows the pioneering work of Burton and Vance (2000) and Stoll et al. (2007) who demonstrated that Nd variability in planktic foraminiferal shells (*Globorotalia menardii*) varied on a glacial/interglacial timescale and was likely related to changes in river flux into the Bay of Bengal due to monsoonal variability. These authors also suggested dust source variability and ocean circulation may have had some influence on Nd isotope values.

In summary, ϵNd of planktic foraminiferal shells may be used to estimate bottom water variability in deep water sequences; however, these types of data have also been used to estimate relative monsoonal fluvial variability off PNG.

4 Evidence for seasonality of the Australian paleomonsoon

As iterated in the previous section, there are many paleoprecipitation indicators and geomorphic features that are related to the Australian paleomonsoon in regions that presently or in the past lay at latitudes where boundary conditions would have been suitable for summer precipitation. However, delineating monsoonal seasonality, and thus differentiating the three types of monsoons, is more difficult. Techniques such as spore pollen transfer functions, coral luminescence analyses, and C3/C4 ratios of marine sediment have been used to document monsoonal seasonality in Australia.

4.1 Terrestrial floral evidence

There are numerous approaches for quantitatively reconstructing seasonal precipitation from fossil palynofloral and macrofloral assemblages including (1) the indicator species approach, (2) the assemblage approach, and (3) the multivariate numerical transfer function approach (Birks and Seppa 2004). The assumption underlying these approaches is that modern-day distributions can be used as a model or analogue for past conditions (i.e., consistent pollen-climate relationships). The transfer function is particularly useful for capturing seasonality of precipitation because it can reconstruct one or more climatic variables (i.e., mean summer rainfall), from a fossil palynofloral assemblage (van der Kaars et al. 2006). The most applied approach, however, involves assigning taxa to floral groups largely based on their present-day ecology (i.e., the nearest living relative approach) and interpreting changes in the visual representation of the major taxa (van der Kaars et al. 2002; Dodson and Macphail 2004; Kershaw et al. 2003; 2007). Notably, the accuracy of estimates derived from the NLR approach depend on

the quality of the modern climate and plant distribution databases, uncertainties in the identification of a fossil taxa and their nearest living relatives, and uncertainties on the total number of taxa within a fossil assemblage (Utescher et al. 2014). NLR methods also do not account for changes in the relative abundance of fossil taxa or long-distance transport of palynomorphs resulting in “mixed” assemblages from different habitats or vegetation zones (Hollis et al. 2019).

In summary, there are several ways to determine seasonal precipitation from palynofloral and macrofloral assemblages. This includes and indicator species approach assemblage analyses and transfer functions. Transfer functions are effective in the estimation of precipitation seasonality and mean summer rainfall reconstructions. The NRL approach assigns taxa to conditions based on their modern ecology, and this method depends on correct fossil identification in modern databases.

4.2 Luminescent layering in corals of the Great Barrier Reef

Evidence of monsoonal freshwater plumes (Fig. 2b) from river catchments adjacent to the Great Barrier Reef is recorded in the annular layers of massive coral skeletons (Lough 2007). Organic material (terrestrial fulvic and humic acids) from wet season runoff is incorporated into bands that can be distinguished from dry season layers (carbonate-rich) using ultraviolet light (Isdale 1984; Lough 2007). Lough (2007) showed a very high correlation between the occurrence of the organic bands and flood events due to monsoonal activity. Combined with high precision ^{14}C dating and historical records, Lough (2007) and Lough et al. (2014) have demonstrated that this technique can be used to obtain high resolution and Holocene to recent decadal climate variability and patterns of monsoonal precipitation off northeast Australia. Lough (2007) showed that rainfall in the region was more extreme and heavier in the twentieth century than in previous centuries prior to the instrumental record.

4.3 The relative abundance of C_4 and C_3 plants in marine cores

There is a strong relationship between seasonal water availability and the relative abundance of C_4 plants in Australia (Murphy and Bowman 2007). One way to ascertain the proportion of C_3 and C_4 vegetation through time includes molecular fossil n -alkanes (Smith and Freeman 2006) which record changes in the proportion of plants using the two main physiological pathways for photosynthesis; C_3 and C_4 (Ehleringer and Monson 1993). An advantage this approach is that n -alkanes are often well-preserved in temporally continuous geological successions that extend across millions of years (Eglington and Logan 1991). A weakness is that reworking can

impact the $\delta^{13}\text{C}$ values of leaf wax n -alkanes in sedimentary records (Baczynski et al. 2019). Despite this, Andrae et al. (2018) used bulk carbonate sediment organic geochemical analyses to measure $\delta^{13}\text{C}$ values of n -alkanes in order to determine the relative abundance of C_4 relative to C_3 plants in offshore northwest Australian to interpret the onset of seasonality and monsoonal activity in the Neogene.

5 Cenozoic history of the Australian paleomonsoon

The temporal framework for terrestrial change provided by the more recent marine records, integrated with continental records from around Australia, supports our use of a “present is the key to the past” approach in interpreting paleoarchives. The addition of these new archives allows us to present a robust Cenozoic history of the Australian paleomonsoon here. Therefore, having described the modern setting of the Australian monsoon in detail in Sect. 1, we describe the history of its variability starting most recently in the Holocene through to its pre-Quaternary record. This synthesis distinguishes records from the *Australian Monsoon* (sensu stricto), the *Quasi-Monsoon*, and the *Pseudo-Monsoon* as classified in Sect. 1 (Fig. 1a, c; Table 1). As there are many more Quaternary records than for the Neogene, we will describe monsoonal history over several time scales: 0 to 25 ka (Figs. 4, 5, 6); 25 to 150 ka (Figs. 7, 8, 9); 150 to 2 Ma (Fig. 10) and 2 Ma to the start of the Neogene (Fig. 11) and consider possible evidence for a Paleogene Australian paleomonsoon.

5.1 The paleomonsoon over the last 25 ka

This section reviews monsoonal and precipitation variability from the LGM to the Holocene to highlight the contrast between the generally drier glacial versus wetter interglacial conditions across northern Australia and the Indonesian Archipelago.

5.1.1 Australian Monsoon (sensu stricto)

Several studies have documented the *Australian Monsoon* (sensu stricto) using different proxies (Fig. 1b, 4). The dominance of pollen with high representation today in modern rainforests at 5°S in the offshore core Site MD98-2175 (Loc. 1, in the Banda Sea, Table 1; Fig. 1, 4; Supp. Fig. 1) suggests wetter conditions after 11 ka compared to the LGM (Kershaw and van der Kaars 2006). The LGM at this site was characterized by significant (seasonal) summer precipitation (pollen transfer function analyses) > 800 mm (Beaufort et al. 2010). In addition, REE/Ca ratios in the planktonic foraminifer *Globigerinoides ruber* suggest increased fluvial runoff in core MD05-2925 (Liu et al. 2015; Loc. 4, Figs. 1b, 4) from 25

Table 1 A list of the locations referred to in the text their age and location (see also Fig. 1a, b)

Australian Monsoon (<i>sensu stricto</i>)—Northern and Central Australia, Indonesia and PNG								
Loc. no.	Oldest ka	Youngest ka	Section type	Lat.	Long.	Location/Site	Indicators	Author
1	150	0	Offshore core	−5.000	133.446	Arafura Sea MD98-2175	Nanofossils and palynomorph, pollen transfer functions	Beaufort et al. (2010)
1	175	0	Offshore core	−5.000	133.446	Arafura Sea MD98-2175	Pollen and charcoal	Kershaw and van der Kaars (2006)
2	12	0	Speleothem	−8.533	120.433	Liang Luar, Flores, Indonesia	trace element and stable isotope ratios	Griffiths et al. (2009)
2	90	80	Speleothem	−8.533	120.433	Liang Luar, Flores, Indonesia	stable isotope ratios	Griffiths et al. (2010)
3	25	0	Offshore core	−8.789	128.641	SO185-18460	Core XRF	Kuhnt et al. (2015)
4	282	0	Offshore core	−9.344	151.46	Off PNG MD05-2925	Rare earth elements Nd/Ca	Liu et al. (2015)
5	10	0	Lakes, swamp	−13.97	136.593	Groote Eylandt, N.T.	Pollen	Donders et al. (2007), Shulmeister (1992), Shulmeister and Lees (1995)
6	300	0	Lake	−17.833	133.517	Lake Woods, Kimberley WA	Lake shorelines and thermoluminescence	Bowler et al. (2001)
	40	0	Lakes, Rivers			Monsoon-influenced northern Australia, compilation	Various	Fitzsimmons et al. (2013)
13	280	0	Rivers	−28.175	137.292	Lake Eyre Basin rivers	thermoluminescence, uranium dating, sediment analyses	Nanson et al. (2008)
14	105	0	Lake	−28.175	137.292	Lake Eyre	OSL TSL of lake shorelines	Cohen et al. (2012, 2015)
14	150	0	Lake	−28.175	137.292	Lake Eyre	Lake shorelines	Magee et al. (2004)
14	250	0	Lake	−28.175	137.292	Lake Eyre	Lake shorelines and thermoluminescence	Fu et al. (2017)
Quasi-Monsoon—Northeast Australia								
	ka	ka						
7	215	0	Offshore core	−16.637	146.304	ODP Site 820 off QLD	Pollen and charcoal	Kershaw and van der Kaars (2006)
7	2000	0	Offshore core	−16.637	146.304	ODP Site 820 off QLD	Pollen	Kershaw et al. (2003)
8	23	0	Lake	−17.159	145.629	Lake Euramoo, NE QLD	Pollen and charcoal	Haberle (2005), Donders et al. (2007)
9	7.3	0	Lake	−17.299	145.583	Quincan Crater, QLD	Pollen and charcoal	Donders et al. (2007)
10	215	0	Lake	−17.367	145.7	Lynch's Crater, QLD	Pollen and charcoal	Kershaw and van der Kaars (2006), Turney et al. (2004)
11	38	0	Swamp	−17.367	145.544	Bromfield swamp, Atherton Tablelands, QLD	XRF, magnetic susceptibility, humification, grain size, macrocharcoal, $\delta^{13}C$ and C/N pollen	Burrows et al. (2016)
12	6	6	Shallow shelf	−19.139	146.834	Great Barrier Reef, Magnetic Island, QLD	Coral (<i>Porites</i> spp.) luminescent lines	Lough et al. (2014)
15	105	0	Lake	−30.667	139.567	Lake Frome	OSL TSL of lake shorelines	Cohen et al. (2012, 2015)
Pseudo-Monsoon—Northwest Australia								
	Oldest ka	Youngest ka	Section type	Lat.	Long.	Location	Proxy/Proxies	Author
16	25	0	Offshore cores	−12.453	121.65	SO185-1879	Core XRF	Kuhnt et al. (2015)

Table 1 (continued)**Pseudo-Monsoon—Northwest Australia**

	Oldest ka	Youngest ka	Section type	Lat.	Long.	Location	Proxy/Proxies	Author
17/18	460	0	Offshore cores	−13.083	121.788	MD01-2378/Site U1483	Core XRF, palynology, foraminifera	Holbourn et al. (2005), Kuhnt et al. (2015), Kawamura et al. (2006), Zhang et al. (2020), Gong et al. (2023)
19	250	0	Offshore core	−13.167	121.586	Offshore NWS, MD98-2167	Pollen and charcoal	Kershaw and van der Kaars (2006)
20	450	0	Offshore core	−15.055	120.435	IODP Expedition 363: Site U1482/SO257-1845	Core XRF	Kuhnt et al. (2015), Pei et al. (2021)
21	45	0	Speleothem	−15.18	128.37	KNI-51, Kimberley region WA	Stable isotopes	Denniston et al. (2013a, b, 2017)
22	25	0	Offshore cores	−15.311	119.501	SO185-18506 Timor Sea, offshore WA	Core XRF	Kuhnt et al. (2015)
23	14.5	0	Outcrop	−15.633	126.389	Black Springs in the Kimberley WA	XRF, spores/pollen, sediment analyses	Field et al. (2017, 2018)
24	300	0	Offshore core	−15.976	117.574	ODP Site 765	Palynology	Gallagher and Wagstaff (2021)
25	45	0	Speleothem	−17.2	125	Ball Gown Cave, Kimberley region WA	Stable isotopes	Denniston et al. (2013a, b, 2017)
26	7	0	Outcrop	−17.422	123.525	Fitzroy River, WA	Sedimentology, palynology	Wywroll et al. (1992)
26	14	0	Outcrop	−17.422	123.525	Fitzroy River, WA	Fluvial & lacustrine stratigraphy	Wywroll and Miller (2001)
27	12000	0	Offshore core	−18.963	117.624	IODP Expedition 356: Site U1463	Core XRF, downhole gamma	Christiansen et al. (2017), Groeneweld et al. (2017)
28	5000	0	Offshore core	−19.887	112.254	ODP Site 762, off NWS	Core XRF	Stuut et al. (2014, 2019), Auer et al. (2020)
29	14	0	Offshore core	−20.214	115.0565	IODP Expedition 356: Site U1461	Core XRF	Ishiwa et al. (2019), Hal-lenberger et al. (2019)
30	14	0	Lake	−20.214	127.447	Lake Gregory WA	Lacustrine stratigraphy	Wywroll and Miller (2001)
30	300	0	Lake	−20.214	127.447	Lake Gregory (Mulan), Kimberley WA	Lake shorelines and thermoluminescence	Bowler et al. (2001), Fitzsimmons et al. (2012)
31	2000	0	Offshore well	−20.294	115.459	Austin-1	Downhole gamma	Gallagher et al. (2014)
32	2000	0	Offshore well	−20.548	115.175	Maitland North-1	Downhole gamma	Gallagher et al. (2014)
33	9000	0	Offshore core	−20.587	112.209	ODP Site 763, off NWS	C3/C4 organic geochemistry	Andre et al. (2018)
34	105	0	Offshore core	−22.046	113.502	Fr10/95-GC17 off Cape Range WA	Pollen, Pollen transfer functions	van der Kaars et al. (2006)
34	34	0	Offshore core	−22.046	113.502	Fr10/95-GC17 off Cape Range WA	Foraminifera, nanofossils, stable isotopes, clay content, sediment composition, pollen	De Deckker et al. (2014)
35	500	0	Offshore core	−22.129	113.502	MD00-2361	Core XRF	Stuut et al. (2014)

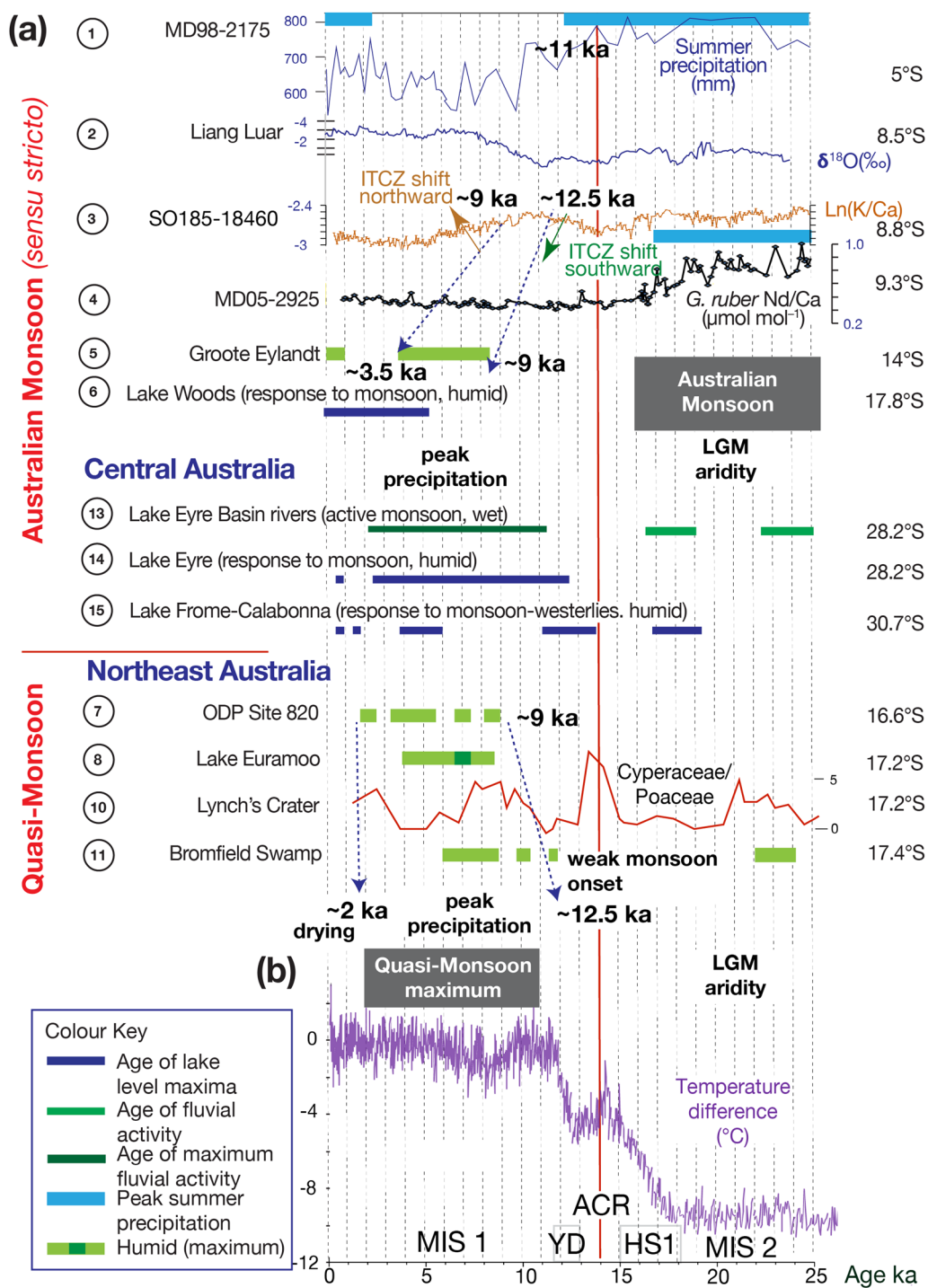


Fig. 4 Records of the late Quaternary to Holocene *Australian Monsoon* (sensu stricto) and *Quasi-Monsoon*: **a** Data from various sites off northern and central Australia (see Table 1 for location and proxy details and Supplementary Fig. 1 for floral data); **b**. EDML (EPICA ice core from Dronning Maud Land) Antarctic ice core δ¹⁸O_{ice} record (EPICA 2006). YD, Younger Dryas, ACR, Antarctic Cold Reversal, HS1, Heinrich Stadial 1. The color key schema and regional classification follows Fitzsimmons et al. (2013).

to 18 ka corresponding to high obliquity insolation when the ITCZ moved southward toward Australia (Kuhnt et al. 2015). Speleothem stable isotope archives at Liang

Luar (Loc. 2, Figs. 1b, 4) suggest wetter conditions during Heinrich stadial 1 (HS 1, 18–15 ka) and MIS (Marine Isotope Stage) 2, drier conditions during the Younger

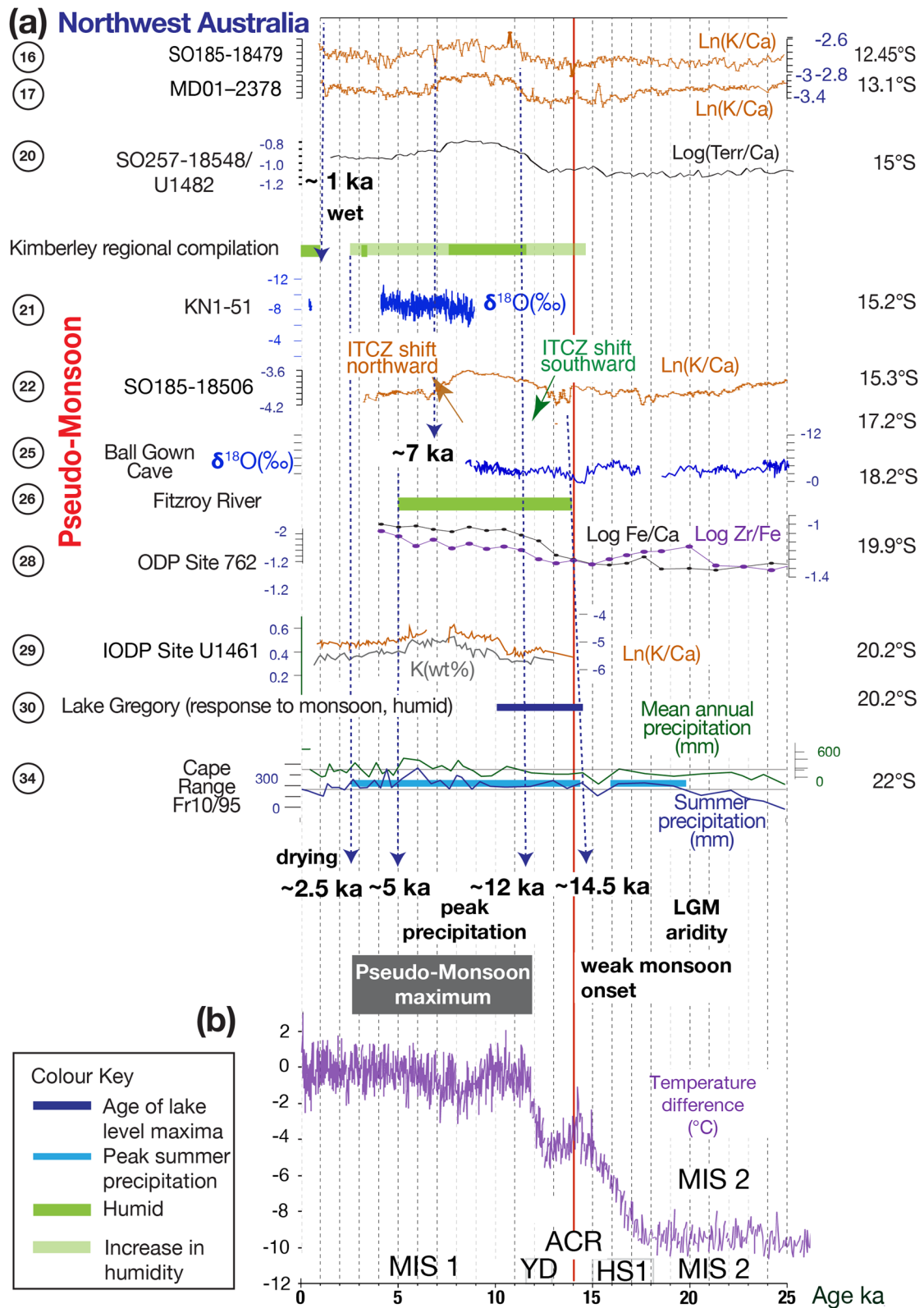


Fig. 5 Records of the late Quaternary to Holocene *Pseudo-Monsoon*: **a** Data from various sites onshore and offshore northwestern Australia (see Table 1 for location and proxy details and Supplementary Fig. 1 for floral data); **b** EDML (EPICA ice core from Dronning Maud Land) Antarctic ice core $\delta^{18}O_{ice}$ record (EPICA 2006). The color key schema and regional classification follows Fitzsimmons et al. (2013).

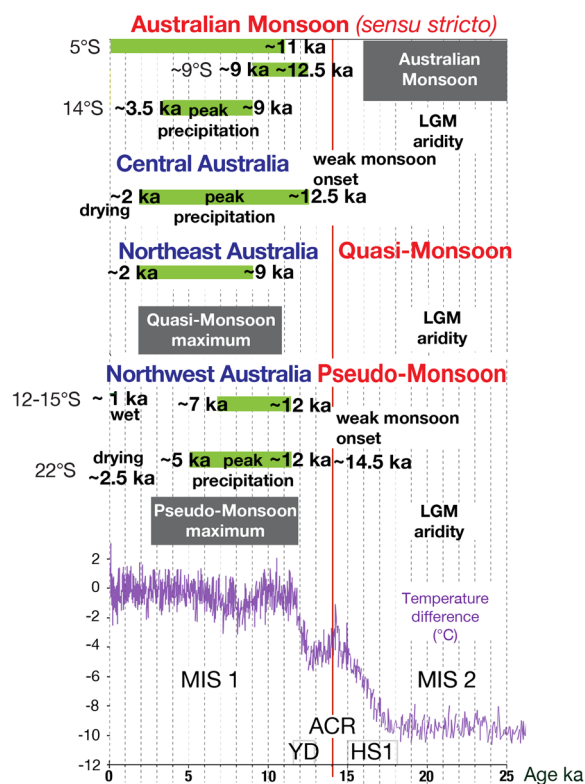


Fig. 6 A summary of the monsoonal and paleoprecipitation records in Figs. 4 and 5.

Dryas (YD ~12 ka) and the Antarctic Cold Reversal (ACR ~14 ka) followed by a gradual Holocene transition to modern monsoonal conditions from 10.5 to 9.5 ka (Griffiths et al. 2009; 2010).

XRF elemental data ratios ($\ln(K/Ca)$) in sediment cores (*Australian Monsoon* (*sensu stricto*) SO185-18460, Loc. 3, Figs. 1, 5 and *Pseudo-Monsoon* cores SO185-18479, Loc. 17, MD01-2378, Loc. 18; Table 1) in a transect across the Timor Sea (Kuhnt et al. 2015), suggest *Australian Monsoon* (*sensu stricto*) and *Pseudo-Monsoon* intensification at the same time as Southern Hemisphere warming and increased greenhouse forcing over Australia after the ACR (15–12.9 ka, Figs. 4, 5). Therefore, an increase in monsoon activity associated with the southward shift of the ITCZ occurred at the same time as the main deglacial atmospheric CO_2 rise from 12.9 to 10 ka. This was followed by a decrease in monsoonal intensity from ~9 to 7 ka as the ITCZ moved northward. Subsequently, drier conditions returned from 8.1 to 7.3 ka.

Vegetation variations revealed in a 10 ka palynofloral record at Groote Eylandt (Loc. 5, Figs. 1, 4) in the Northern Territory (Shulmeister 1992; Shulmeister 1992; Donders et al. 2007) suggest an increase in precipitation from 8.4 to 4.5 ka with the onset of modern ENSO dynamics and drier conditions followed by increased precipitation

at ~1 ka. The existence of elevated shorelines at Lake Woods (Loc. 6, Figs. 1, 4) suggests lake expansion due to an increased monsoon from 6.5 ka (Bowler et al. 2001). Evidence of enhanced fluvial activity and ephemeral lake shoreline expansion and contraction in central Australia are used to interpret *Australian Monsoon* (*sensu stricto*) variability (Fig. 4). Lake Eyre in central Australia (Loc. 14, Figs. 1, 4) receives significant precipitation during the monsoonal season source primarily from the northern Australia with lesser river input from northeast Australia. The rivers (Loc. 13, Figs. 1, 4) that feed into this mega lake and its shoreline sediments have been dated using thermoluminescence (TSL) and uranium dating techniques (Nanson et al. 2008; Fitzsimmons et al. 2013). This suggests possible monsoonal conditions prevailed during MIS2 at ~23 ka and ~17 ka during HS1. Subsequently, fluvial activity was most intense from ~11 to 2 ka with a maximum ~5 ka. The age of the highest elevation shorelines of Lake Eyre is used to interpret monsoonal intensity. TSL and OSL techniques suggest Lake Eyre infill from ~12.5 ~2 ka (Magee et al. 2004; Fitzsimmons et al. 2013; Cohen et al. 2012; Fu et al. 2017). The more southerly Lake Frome (Loc. 15, Figs. 1, 4) is influenced by both the monsoon and westerlies. The age of the shoreline of this lake reveals intermittent precipitation maxima ~18, 12.5, 5 and 0.5 ka (Cohen et al. 2012; 2015; Fitzsimmons et al. 2013).

5.1.2 Quasi-Monsoon

Northeast Australian palynofloral records are used to interpret *Quasi-Monsoon* variability (Fig. 4) over the last 25 ka. Peaks in rainforest gymnosperm and angiosperm abundance in the marine archive of ODP (Ocean Drilling Program) Site 820 (Loc. 7, Table 1, Figs. 1, 4; Supp. Fig. 1) suggest maximum precipitation from ~9.5 (monsoon onset) to 1.5 ka followed by drier conditions (Kershaw and van der Kaar 2006). The influx of rainforest taxa in Lake Euramoo (Loc. 8, Figs. 1, 4) since 8.7 ka denotes monsoonal intensification reaching a maximum from 7.3 to 6.3 ka (Haberle 2005; Donders et al. 2007) thereafter drier conditions prevailed from 5 ka possibly indicating the onset of El Niño related climate variability. A high ratio of Cyperaceae (sedge) to Poaceae (grass) is interpreted to reflect wetter conditions (monsoonal precipitation) in the palynofloral record of Lynch's Crater (Loc. 10, Fig. 4; Supp. Fig. 1, Turney et al. 2004; Kershaw and van der Kaar 2006). Several wet maxima occur during MIS 2 (21–23 ka), the ACR and from 10 to 7 ka with a later wet period ~2 ka (Turney et al. 2004; Muller et al. 2008). The wet maxima events are interpreted to be related to millennial-scale perturbations when the ITCZ periodically migrated further south across northeastern Australia during Heinrich events (Turney et al. 2004; Muller

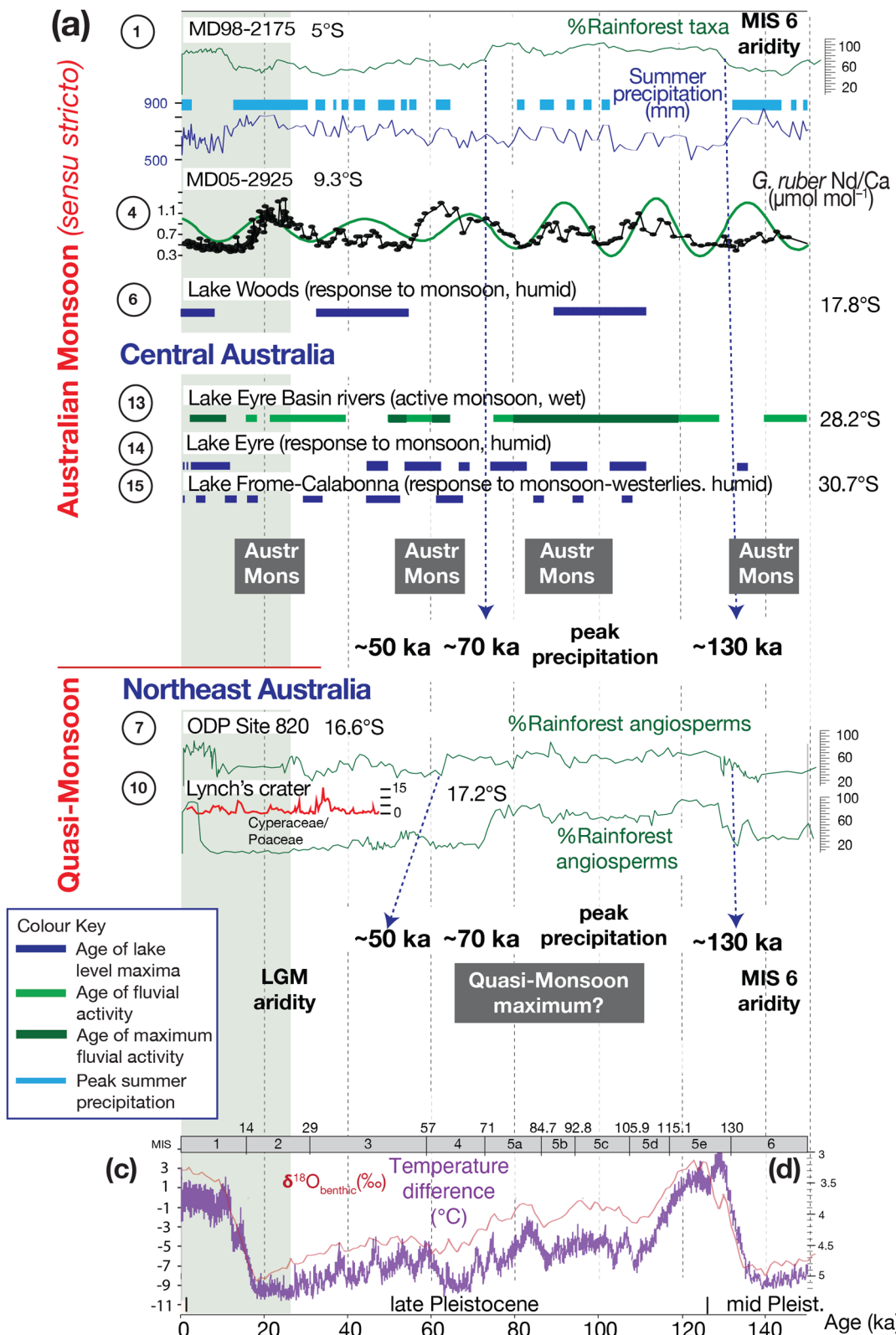


Fig. 7 Records of the middle to late Pleistocene *Australian Monsoon* (sensu stricto) and *Quasi-Monsoon*: **a** Data from various sites of northern and central Australia (see Table 1 for location and proxy details and Supplementary Fig. 1 for extra palynofloral data); **b** The purple line is the EDML (EPICA ice core from Dronning Maud Land) Antarctic ice core $\delta^{18}\text{O}_{\text{ice}}$ record (EPICA 2006). The pink line the LR04 isotope stack (Lisiecki and Raymo 2005). The color key schema and regional classification follows Fitzsimmons et al. (2013).

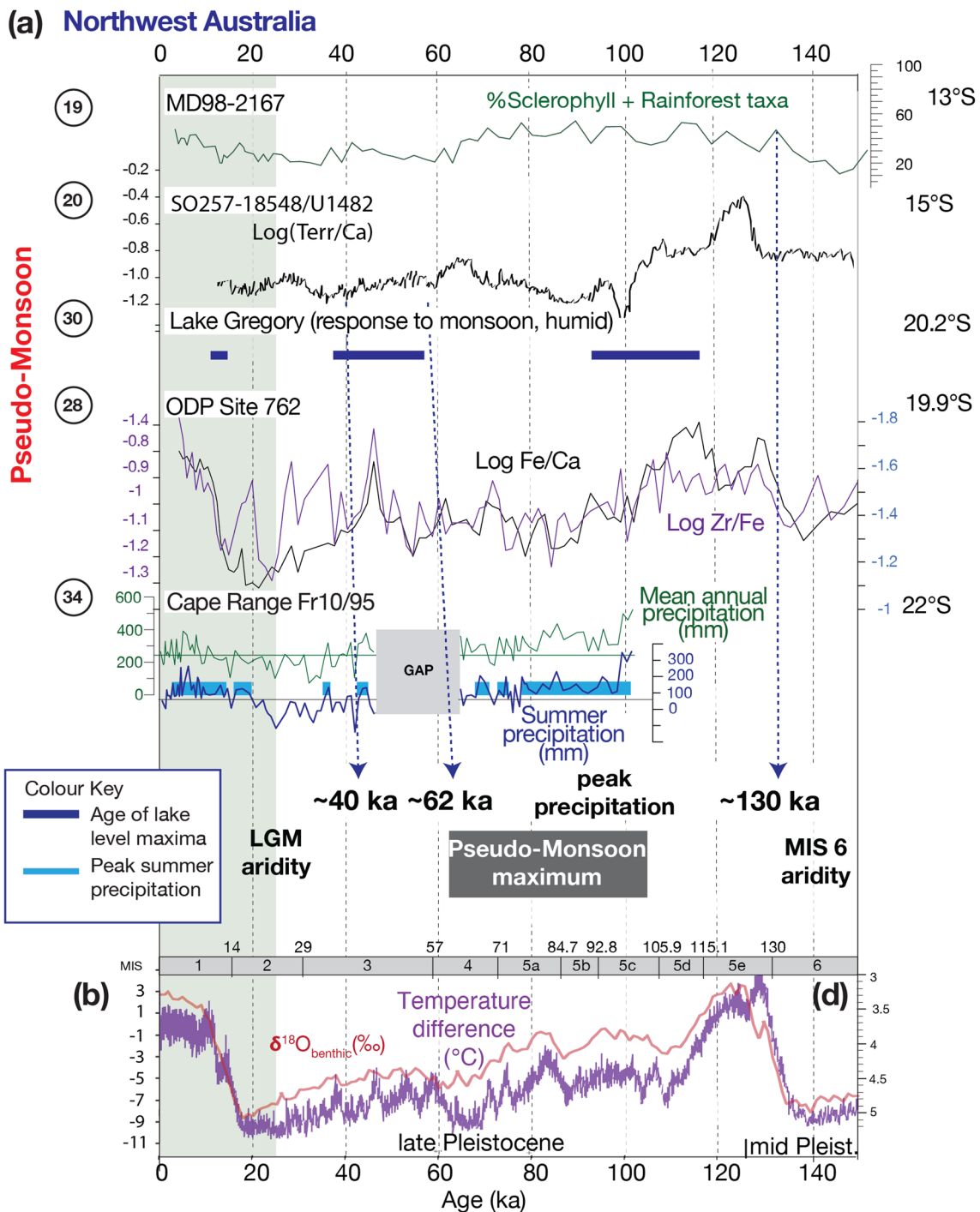


Fig. 8 Records of the middle to late Pleistocene *Pseudo-Monsoon*: **a** Data from various sites onshore and offshore northwestern Australia (see Table 1 for location and proxy details and Supplementary Fig. 1 for extra palynofloral data); **b** The purple line is the EDML (EPICA ice core from Dronning Maud Land) Antarctic ice core $\delta^{18}O_{\text{ice}}$ record (EPICA 2006). The pink line the LR2004 isotope stack (Lisiecki and Raymo 2005). The color key schema and regional classification follows Fitzsimmons et al. (2013).

et al. 2008). Multiproxy analyses (palynofloral, $\delta^{13}C$, C/N, magnetic susceptibility, humification, core XRF scanner and grain size analyses) of the nearby Bromfield Swamp

sequence (Loc. 11, Figs. 1, 4) reveal a broadly similar precipitation record to Lynch’s Crater (Burrows et al. 2016) with maxima at ~22 ka and from 11.5 to 6 ka.

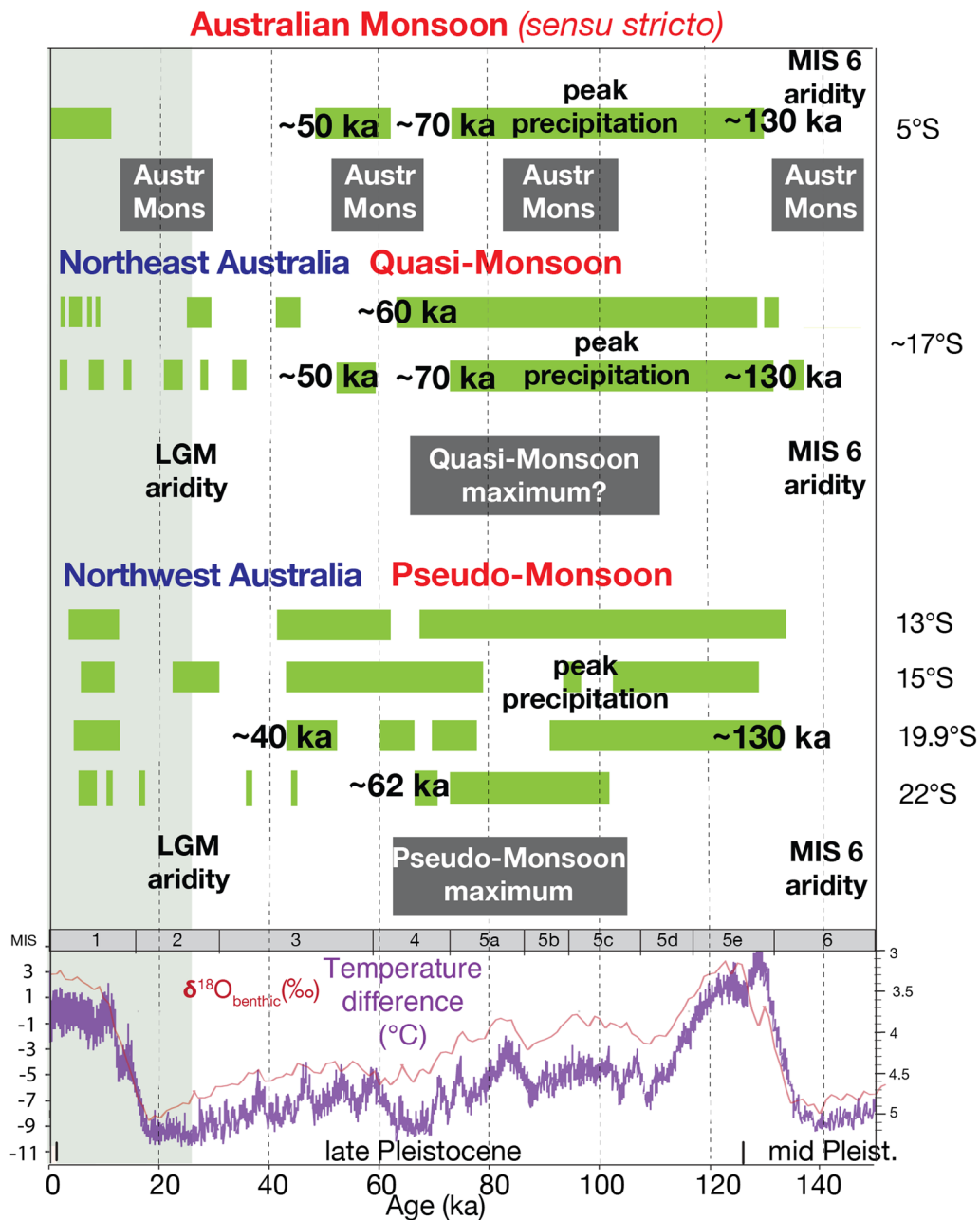


Fig. 9 A summary of the monsoon and paleoprecipitation records shown in Figs. 7 and 8.

5.1.3 Pseudo-Monsoon

Offshore and onshore archives preserve evidence of the *Pseudo-Monsoon* in Northwest Australia (Fig. 1). This region includes the Kimberley Fitzroy River catchment and the Carnarvon De Grey and Fortescue River catchments (Fig. 1a):

(a) Kimberley Fitzroy river catchment

XRF core scanner $\ln(K/Ca)$ data from SO185-1879 and MD01-2378 (Loc. 16, 17, Table 1, Figs. 1, 5) suggest a

precipitation maximum ~12 to 7 ka (Kuhnt et al. 2015). Further south at IODP (International Ocean Discovery Program) Site U1482/SO257-1848 (Loc. 20, Figs. 1, 5), a similar onset of ~12 ka was followed by a longer wetter period until ~5 ka with some precipitation from MIS 2 ~24 ka to MIS 1 (~14 ka) (Kuhnt et al. 2015; Pei et al. 2021).

Speleothem (stable isotope) and sediment/XRF scanner/palynofloral analyses of spring deposits in the

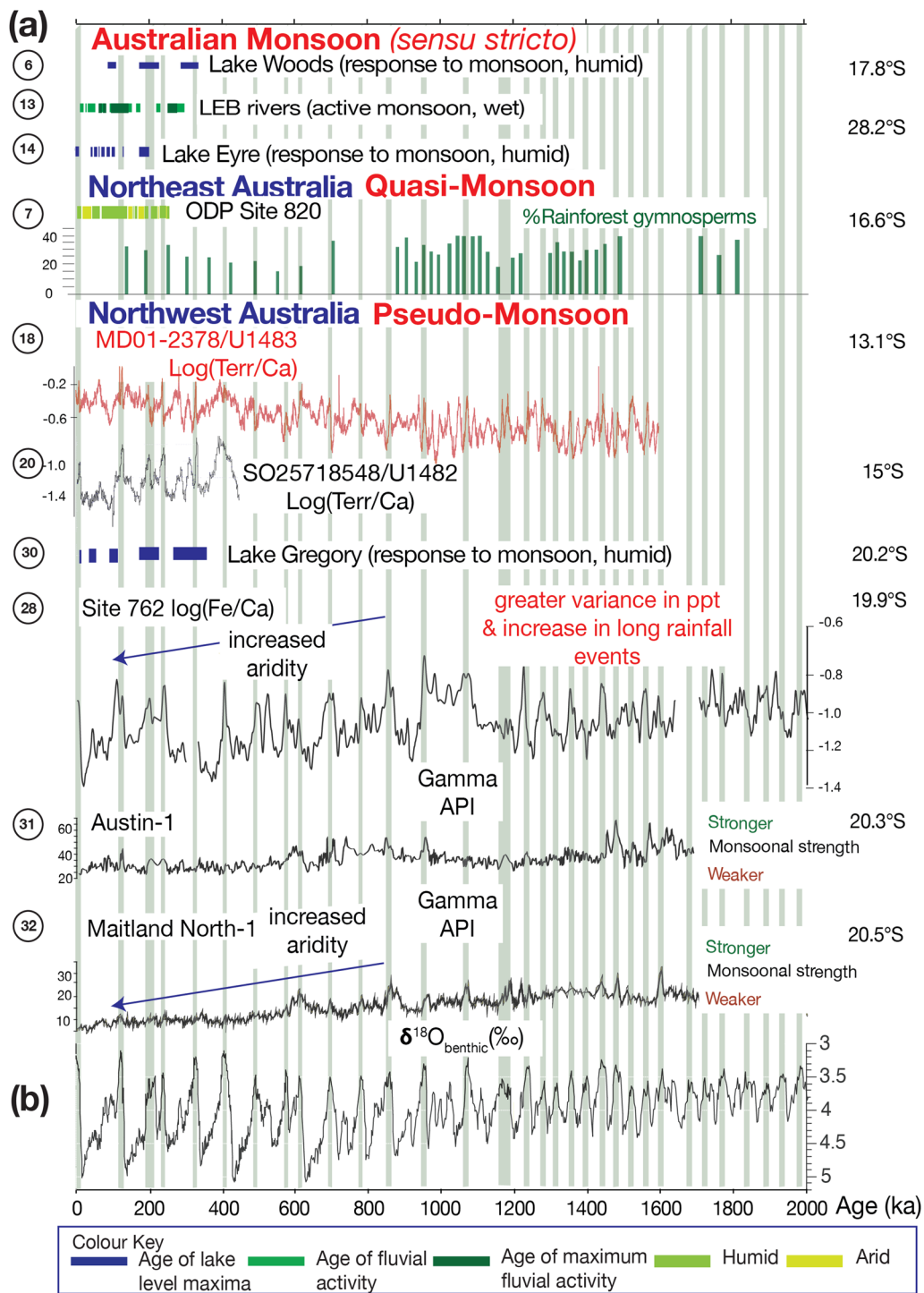


Fig. 10 Records of the early to middle Pleistocene *Australian Monsoon* (*sensu stricto*), *Quasi-* and *Pseudo-Monsoon*: **a** Data from various sites onshore and offshore northern and central Australia (see Table 1 for location and proxy details and Supplementary Fig. 1 for floral data); **b** The LR2004 isotope stack (Lisiecki and Raymo 2005). The color key schema and regional classification follows Fitzsimmons et al. (2013).

Kimberley region (Loc. 21, 23, Figs. 1, 5) reveals a detailed monsoonal history over the last 25 ka (Deniston et al. 2013a, 2013b, 2017; Field et al. 2017, 2018).

Negative oxygen isotope minima in the well-dated Ball Gown Cave and KN1-51 speleothems suggests maximum precipitation from 9 to 4 ka with rainfall peaks

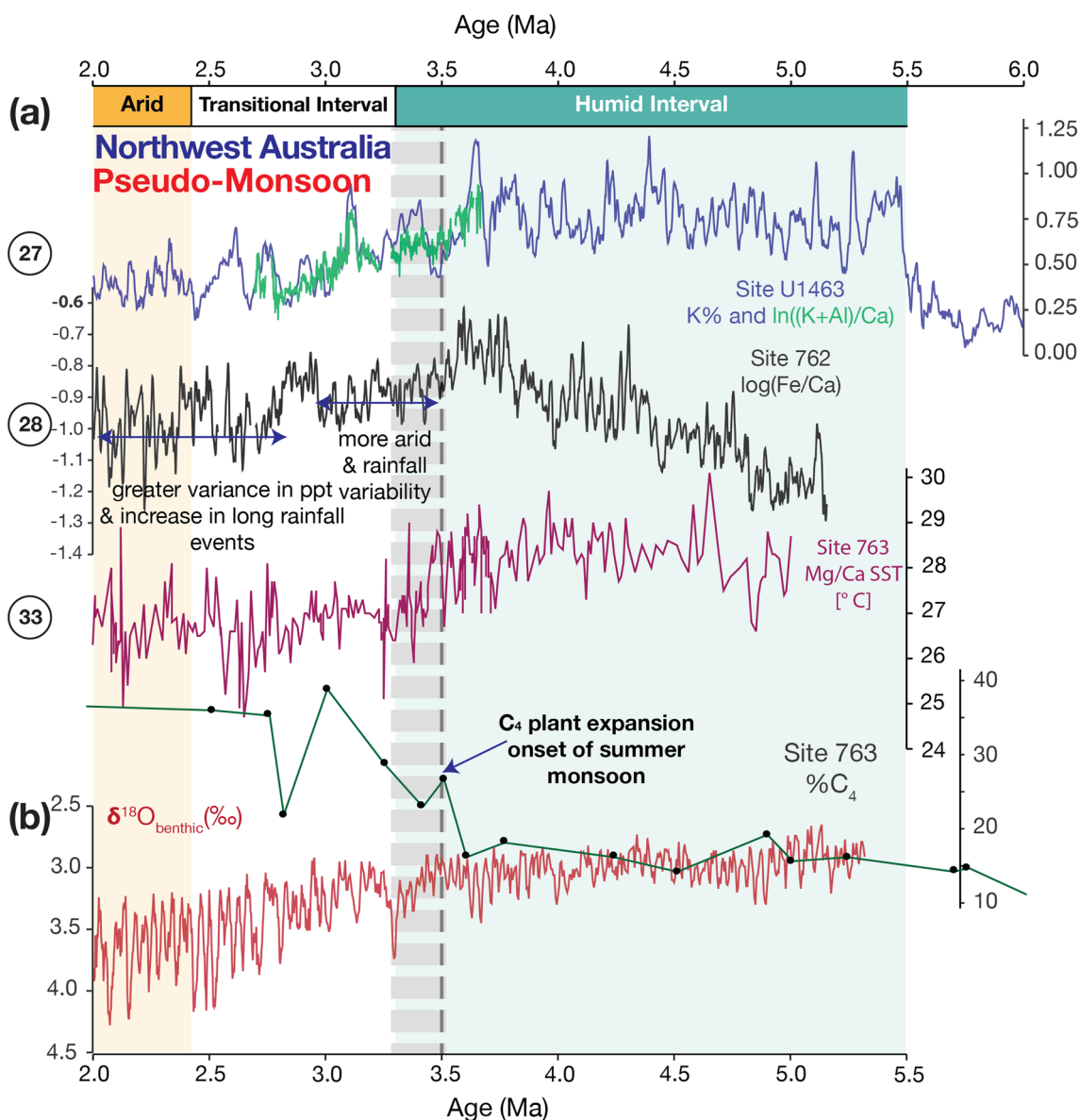


Fig. 11 **a** Records of the Neogene to Quaternary hydroclimate off northwest Australia adapted from Auer et al. (2020), see Table 1 for location and proxy details for each site. The age model for ODP Site 762B log (Fe/Ca) core XRF data (Stuut et al. 2019) is revised by Auer et al. (2020). The data from 5.5 to 2 Ma are compared with records from ODP Hole 763A (Karas et al. 2009; 2011; revised by O'Brien et al. 2014), as well as terrigenous influx data from Site U1463 (Auer et al. 2019; Christensen et al. 2017) with K% data updated to the most recent age model of Auer et al. (2019); The % C₄ plants from ODP Site 763 is from Andrae et al. 2018; **b** The LR04 isotope stack (Lisiecki and Raymo 2005).

during HS 1 (~16 ka) and ~24 ka (Denniston et al. 2013a, 2013b, 2017). A multiproxy synthesis (Field et al. 2018) including these speleothem data with spring deposits (Black Springs (15.633°S, 126.389°E), Fern Pool (15.937°S, 126.284°E), and Gap Springs (16.404°S, 126.134°E) in the Kimberley region (Figs. 1, 5) suggests the following history: (i) Minimal monsoonal activity prior to 14.5 ka, (ii) a weak yet active summer monsoon from 14.5 to 11 ka, (iii) active strong monsoonal activity from 11 to 7.5 ka

BP, (iv) weakening summer monsoon from 7.5 to 2.6 ka, and (v) minimal or inactive summer monsoon from 2.6 to 1 ka followed by modern active summer monsoon conditions over the last 1 ka. Offshore from the Kimberly region, XRF analyses of SO185-18506 (Loc. 22, Figs. 1, 5) suggest a precipitation peak from 12.5 to 8 ka (Kuhnt et al. 2015) associated with a southerly migration of the ITCZ, with rainfall reduction due to a northerly shift of the ITCZ after 8 ka.

Sedimentary facies and palynofloral analyses of the fluvial records of the Fitzroy River (Loc. 26, Figs. 1, 5) south of the Kimberley region suggests wetter conditions initiated at the start of MIS 1 ~14 ka and persisted until at least 5 ka (Wyrwoll et al. 1992; Wyrwoll and Miller 2001). Stratigraphic analyses and thermoluminescence dating of the shorelines of Lake Gregory (Loc. 30, Figs. 1, 5) suggest peak monsoon lake levels from ~16.5 to ~11 ka (Wyrwoll and Miller 2001; Bowler et al. 2001).

(b) Carnarvon De Grey and Fortescue River catchments

Offshore at ODP Site 762 XRF core scanner data (Loc. 28, Table 1, Figs. 1, 5, 6) record a Holocene monsoon onset of ~12.5 ka (Stuut et al. 2019; Auer et al. 2020). XRF analyses of a marine archive (IODP Site U1461, Loc. 29, Figs. 1, 5) offshore from Lake Gregory suggest peak rainfall from 10.5 to 6 ka (Ishiwa et al. 2019). Further south at Cape Range (Site Fr10/95, Loc. 33, Figs. 1, 5), transfer functions applied to palynofloral records are used to interpret the wettest period and estimate summer precipitation (van der Kaars et al. 2006; De Deckker et al. 2014). These data reveal summer rainfall over 100 mm per annum from 20 to 2.5 ka with minima at ~15 ka. This record also suggests periodic rainfall maxima at ~14 ka and from 8 to 4.5 ka (Fig. 5).

5.1.4 Australian monsoon 25–0 ka synthesis

Significant research has been carried out on northern Australian climate of this interval. In general, all records show increased Holocene (MIS 1, <12 ka) precipitation following the arid conditions of the LGM (Figs. 4, 5, 6). In particular, the ITCZ was north of continental Australia from the LGM to the YD (Fig. 3) when *Australian Monsoon* (sensu stricto) seasonality was well expressed in marine records at ~5° and 9.3°S (Figs. 4, 6), while the rest of Australia was typically arid. There is a diachroneity in the precipitation records from the *Australian Monsoon* region from ~9 to 14°S (Fig. 4) suggesting that the ITCZ may have shifted southward during the time followed by a northward shift (Figs. 4, 6) and peak precipitation from 9 to 3.5 ka. At present, there are an insufficient number of records in this region to spatially map ITCZ location with more certainty. The timing of infill of the monsoonal Lake Woods does not match any other *Australian Monsoon* (sensu stricto) records (Figs. 4, 6). This may be related to dating problems or gaps in the sequence as its chronology has not been updated since 2001 (Bowler et al. 2001).

Filling of the monsoonal Lake Eyre and rejuvenation of Lake Eyre Basin rivers suggests the *Australian Monsoon* (sensu stricto) intensified from ~12 ka. Other terrestrial records from ~17°S (Fig. 4) show variable onset times of wetter periods, which may be related to the presence of gaps in these sequences and errors in carbon dating. Nevertheless, these records show precipitation maxima from

~9 to ~2 ka. There is a general trend to drying conditions after ~2 ka, suggesting a reduction in Quasi-Monsoon intensity (Figs. 4, 6).

The *Pseudo-Monsoon* record is more extensively sampled via offshore IODP and ODP archives with limited terrestrial records in lakes, caves and rivers (Figs. 5, 6). Most records show maximum precipitation from 12.5 ka with limited evidence of a weaker monsoon onset after 14.5 ka. North of 15°S most records show a decrease in precipitation at ~7 ka and this has been suggested to be related to a northward shift in the ICTZ (Kuhnt et al. 2015). However, south of this latitude peak precipitation persists until ~5 ka. This diachroneity may be related to errors in dating, gaps and the time resolution of the records. For example, the fluvial sequences in the Fitzroy catchment are likely to have significant gaps and have not been investigated since 2001 (Wyrwoll et al. 1992; Wyrwoll and Miller 2001). Similarly, the age of monsoonal Lake Gregory has not been investigated since this time (Bowler et al. 2001). Other records such as ODP Site 765 are not sampled in as much resolution as other more northerly marine archives (Figs. 5, 6). Overall, the records show a *Pseudo-Monsoon* maximum from 12 to 2.5 ka followed by a reduction in monsoonal intensity to present with a possible wetter period after 1 ka.

5.2 Middle to late Pleistocene (25–150 ka) monsoon

5.2.1 Australian Monsoon (sensu stricto)

Several studies have documented the longer-term Quaternary variability of the *Australian Monsoon* (sensu stricto) using different proxies (Figs. 1, 6). Rainforest pollen dominate core MD98-2175 (Loc. 1, Table 1, Figs. 1, 6; Supp. Fig. 1), suggesting wetter periods during MIS 5 (130–70 ka) and the end of MIS 3 (~35 ka) (Kershaw and van der Kaars 2006). Pollen transfer functions suggest intermittent summer precipitation maxima (> 700 mm) from the end of MIS 4 (57 ka) to MIS 2 (~14 ka), during MIS 6 (~140 ka) and MIS 5c-a (71–106 ka) (> 800 mm, Beaufort et al. 2010). REE Nd/Ca ratios in *Globigerinoides ruber* in core MD05-2925 (Liu et al. 2015; Loc. 4, Figs. 1, 7) continue the trend from 0 to 25 ka with higher ratios corresponding to high obliquity insolation periods. Additional lake shoreline heights from Lake Woods (Loc. 6, Figs. 1, 7) suggests increased monsoonal influence from MIS 5d (~106 ka) to MIS 3 (~40 ka) (Bowler et al. 2001).

The fluvial and lacustrine records of central Australia extend the monsoonal record for Lake Eyre beyond 150 ka (Loc. 13, 14, Figs. 1, 7). Peak fluvial activity is interpreted from 120 to 80 ka with lesser yet active intermittent fluvial activity prevailed from MIS 6 (130 ka), to MIS 3/2 (~30 ka) (Nanson et al. 2008; Fitzsimmons et al. 2013).

Lake Eyre shorelines have been dated using OSL to MIS 6 (143 ± 15 ka), and MIS 5 from 130 ± 16 ka to 113 ± 20 ka (Fu et al. 2017). Using these dates, Fu et al. (2017) correlate high lake levels to possible warm interglacial and cold glacial periods with the wettest times occurring between interglacial and glacial stages. This contrasts with previous interpretations (Magee et al. 2004) that maximum lake levels represent the warmest interglacial conditions. The lack of any clear association between lake levels and insolation peaks suggests to these authors that orbital forcing was not a primary control for the *Australian Monsoon* (sensu stricto) and that it may have been influenced by abrupt millennial events at least to ~ 200 ka (Fu et al. 2017); however, further similarly dated lake shoreline deposits would be needed to confirm this. This contrasts with previous interpretations that suggest that the Australian paleomonsoon was precession/obliquity controlled (Wyrwoll et al. 2007, 2012; Holbourn et al. 2005). The age of the paleoshorelines of Lake Frome (Loc. 15, Figs. 1, 7) occasionally correlate with those of Lake Eyre, suggesting that these lakes periodically amalgamated to form a mega lake during peak monsoonal conditions (Cohen et al. 2012; 2015). Similar to Lake Eyre, these short-duration Lake Frome maxima also do not clearly align with insolation, possibly due to a millennial control (cf. Fu et al. 2017) and to the intermittent influence of the westerlies (Cohen et al. 2012, 2015; Fitzsimmons et al. 2013) on this lake catchment especially during wetter periods when they were out of phase with those of Lake Eyre. Nevertheless, the ages (with +/-errors) of these shorelines (represented by the full duration of the dark blue horizontal bars in Figs. 7) obtained by Fu et al. (2017) and Cohen et al. (2012; 2015) make it difficult to fully establish relationships to millennial-scale monsoonal processes.

5.2.2 Quasi-Monsoon

Two >150 kyr *Quasi-Monsoon* palynofloral records have been analyzed from onshore and offshore northeast and central Australia (Fig. 7). Rainforest gymnosperms and angiosperms are most common from MIS 5e (~ 130 ka) to MIS 4 (~ 60 ka) at ODP Site 820 (Loc. 7, Table 1, Figs. 1, 7; Supp. Fig. 1) with minor peaks at ~ 30 ka and 55 ka (Kershaw and van der Kaar 2006). At Lynch's Crater (Loc. 10, Fig. 7; Supp. Fig. 1), high ratios of Cyperaceae (sedge) to Poaceae (grass) suggest intermittent short periods of increased monsoonal precipitation during MIS 3 (~ 30 ka) and MIS 2 (~ 20 ka) (Turney et al. 2004; Kershaw and van der Kaar 2006).

5.2.3 Pseudo-Monsoon

Several ≥ 150 kyr duration offshore archives and one lake record preserve evidence of the *Pseudo-Monsoon* in

Northwest Australia. Palynofloral data from Site MD98-2167 (Loc. 19, Table 1, Figs. 1, 8; Supp. Fig. 1, Kershaw and van der Kaars 2006) suggests wetter interglacial conditions at this site from the end of MIS 6 (103 ka) to the beginning of MIS 4 (71 ka) whereas drier conditions prevailed during MIS 6 and MIS 3 and 2. Core XRF log (Terr/Ca) data (Terr = all elements interpreted to be derived from terrestrial sources, e.g., Si, Al, Fe, K and Ti; cf. Pei et al. 2021) from IODP Site U1482/SO257-1848 (Loc. 20, Figs. 1, 8) reveals a similar pattern to MD98-2167 with wetter conditions near the start of MIS 5 (130 ka) with occasional drier phases from MIS 5c to 5a and during MIS 3 (~ 45 ka) (Kuhnt et al. 2015; Pei et al. 2021). The height of paleoshorelines of Lake Gregory (Loc. 29, Figs. 1, 8) suggests precipitation peaked during MIS 3 (~ 45 ka) and MIS 5b-d (115–85 ka) (Bowler et al. 2001). Further south at ODP Site 762 (Loc. 28, Figs. 1, 7) XRF log Zr/Fe and log Fe/Ca data suggests that these wetter and drier phases persisted at similar times (Stuut et al. 2019; Auer et al. 2020). A 100 ka palynofloral climate archive west of the Cape Range Peninsula (Core GC17, Fr10/95, Loc. 34, Figs. 1, 8) (van der Kaars and De Deckker 2002; van der Kaars et al. 2006) (Fig. 1) represents the southern extent of the (modern) Australian summer *Pseudo-Monsoon*. Pollen transfer functions indicate a marked increase in summer rainfall and monsoonal activity from MIS 5c (106 ka) to MIS 4 (57 ka) when annual precipitation was relatively high with short periods of increased summer precipitation in MIS 3 (~ 40 ka, van der Kaars et al. 2006) prior to a drier MIS 2.

5.2.4 Australian monsoon 150-25 ka synthesis

As mentioned previously, longer-term pre-25 ka records of the Australian monsoon are limited and dominated by offshore marine archives (Figs. 7, 8, 9). All records show maximum precipitation periods between ~ 130 ka and ~ 70 – 62 ka (Figs. 7, 8, 9) with more arid glacial periods (LGM and after ~ 40 – 50 ka and MIS 6 prior to 130 ka). Estimates of summer precipitation in the *Australian Monsoon* (sensu stricto) region from 5 to 9°S (Figs. 7, 9) suggest periodic intermittent monsoonal activity, possibly related to obliquity with peak monsoon during glacial periods. Similarly, periods of Lake Eyre monsoon related fluvial activity and the presence of lake shorelines show a highly variable temporal distribution (Figs. 7, 9) with a possible minimum during MIS 5e (130–115 ka). Overall, the correlation between the terrestrial and marine archive *Australian Monsoon* (sensu stricto) events is not clear, likely due to the intermittent nature of terrestrial records and problems with dating. Only two archives of the *Quasi-Monsoon* have been investigated beyond 25 ka, whereby the long-term history of this monsoonal system is less well-constrained. The *Pseudo-Monsoon* is better

constrained off the NW Australian shelf (Figs. 8, 9) with peak summer precipitation occurring from 100 to 57 ka and at ~40 ka at Cape Range. However, the archive at this locality does not extend beyond 100 ka.

5.3 Early to middle Pleistocene (150 ka to 2 Ma) Australian monsoon

5.3.1 Australian Monsoon (*sensu stricto*)

Terrestrial records of the *Australian Monsoon* (*sensu stricto*) do not extend beyond 300 ka. Evidence is sparse in central Australia with Lake Eyre river sediment records only extending to 280 ka (Nanson et al. 2008) and Lake Eyre shoreline archives until 250 ka (Fu et al. 2017). These records suggest an active monsoon from MIS 7 to MIS 6 (~180 ka, Fu et al. 2017) when “paleo” Cooper Creek flow was 5 to 7 times greater than today (Nanson et al. 2008). Further fluvial maxima occur at the MIS 8/MIS 7 boundary (~240 ka, Nanson et al. 2008). Further north, maxima in Nd/Ca ratios in *Globigerinoides ruber* in core MD05-2925 (Loc. 4, Table 1, Fig. 1) correlate to insolation peaks until at least 280 ka (Liu et al. 2015) leading these authors to suggest that the position of the ITCZ moved southward to the Australian continent (to the Monsoon Shear line, Figs. 1, 2) during high obliquity phases and migrated toward the equator during low obliquity times (Liu et al. 2015). Estimates of high lake levels in Lake Woods over the last 300 ka suggest elevated levels broadly during interglacial times (Loc. 6, Figs. 1, 10; Bowler et al. 2001) suggesting a temporal relationship between warmer interglacial periods and wetter monsoonal conditions; however, as mentioned previously, these archives need further investigation since they were last dated in 2001 (Bowler et al. 2001).

In the absence of older records, it is necessary to investigate offshore archives to interpret precipitation variability related to monsoonal runoff from the Australian continent over the last 2 Ma.

5.3.2 Quasi-Monsoon

A sparsely sampled palynological record from ODP Site 820 extends the *Quasi-Monsoon* record back to 2 Ma (Fig. 10, Table 1, Kershaw et al. 2003). The relative percentage of rainforest gymnosperms is relatively high prior to 1 Ma and lower in the period from 600 to 400 ka reflecting the drying and increased aridity of the continent.

5.3.3 Pseudo-Monsoon

More complete archives of the *Pseudo-Monsoon* are sampled in the cored sequences of offshore northwest Australia (Fig. 1b). Strong changes in monsoonal strength between interglacial and glacial periods during the middle Pleistocene have been interpreted off northwest

Australia where enhanced monsoonal (wet) conditions during interglacial periods alternate with weaker monsoon (dry/arid) during glacials (Kawamura et al. 2006; Gallagher et al. 2014; Stuut et al. 2014, 2020; Gallagher and Wagstaff 2021).

Trends in foraminiferal and geochemical data from Site MD01-2378 (Loc. 17, Fig. 1) match the 25°S summer insolation curve, suggesting a strong eccentricity and precessional control on productivity variations due to monsoonal wind pattern variability (Holbourn et al. 2005) over the last 460 ka. Core scanning XRF log(Terr/Ca) and other geochemical data from a 1600 ka record at IODP Site U1483 (Loc. 18, Table 1, Figs. 1, 10) reveal monsoonal precipitation increased markedly during terminal part of glacials attributed to a combination of precession minima and obliquity maxima after the onset of high-amplitude glacial/interglacial cycles at ~1 Ma (Gong et al. 2023), whereas these authors suggest that prior to this, monsoonal rainfall intensity was paced by precessional cycles. Similar XRF log(Terr/Ca) data from a 460 ka record in SO257-18548 and IODP Site U1482 (Loc. 20, Table 1, Figs. 1, 10) are interpreted to reflect increased precipitation and terrestrial influx during interglacial periods with peak monsoon correlating to $p\text{CO}_2$ maxima during austral (precessional) insolation maxima during MIS 7 (200, 220 and 240 ka), MIS 8 and MIS 9 (280, 305, and 330 ka) due to the southward migration of the ITCZ (Kuhnt et al. 2015; Pei et al. 2021). Further south at ODP Site 762 (Loc. 28, Figs. 1, 10), XRF log(Fe/Ca) data reflect a strong variance in precipitation and elevated long rainfall events from 2 to 1 Ma with a switch to drier conditions after this time (Stuut et al. 2019; Auer et al. 2020).

Onshore, elevated lake levels at Lake Gregory (Loc. 30, Figs. 1, 10) are estimated to coincide with interglacial periods over the last 400 ka (Bowler et al. 2001). Directly offshore from Lake Gregory, two well sections (Austin-1, Maitland North-1; Loc. 31, 32, Figs. 1, 10) preserve evidence of terrestrial influx related to relative monsoonal variability back to 2 Ma (Gallagher et al. 2014) in downhole log gamma data. Peaks in green clayey sand (increased terrestrial siliciclastic input) predominated during interglacial wetter conditions (due to monsoonal sediment plumes from the De Grey River, as described by Gallagher et al. 2014; Gallagher and Wagstaff 2021), whereas carbonates with abundant oolites (and minimal siliciclastics) prevailed during the drier glacial phases (where the ooids represent supersaturated high alkalinity conditions, Gallagher et al. 2018), as conditions became more arid. The decrease in Australian monsoonal intensity over the last 1 Ma was accompanied by increased alkalinity and carbonate supersaturation due to enhanced aridification of northwestern Australia (Gallagher et al. 2014; 2018). Other evidence of increased aridity in

Western Australia is the initiation and expansion of the dune fields in the monsoon-influenced Simpson Desert in central Australia around one million years ago (Fig. 1b; Fujioka et al. 2009; Fujioka and Chappell 2010).

5.3.4 Early to middle Pleistocene (150 ka to 2 Ma) Australian monsoon synthesis

There are limited terrestrial records of the Australian Monsoon (*sensu stricto*) that extend back to 300 ka preserved in the Lake Eyre shoreline sediment archives. This suggests active monsoon conditions prevailed from MIS 7 to MIS 6 (~180 ka) when Cooper Creek flow was much higher than today. Offshore PNG cyclic variations in Nd/Ca ratios in foraminiferal shells suggest that the ITCZ moved southward during obliquity phase until at least 280 ka. Lake Wood levels were elevated during interglacial periods suggesting a possible relationship between increased monsoonal conditions and warmer climate phases; however, the chronology of the shorelines of this lake needs improvement. A limited palynological record from ODP Site 820 extends the Quasi-Monsoon back to at least 2 Ma, showing a higher percentage of rainforest gymnosperms prior to 1 Ma, with a reduction from 600 to 400 ka, suggesting increased aridity. Offshore northwest Australia, several sediment cores reveal changes in Pseudo-Monsoon strength between glacial and interglacial periods. Increased monsoon conditions during interglacial periods alternated with drier glacial periods. The record from many sites suggests monsoonal precipitation reached a maximum during interglacial periods, often correlating with pCO₂ maxima and the southward migration of the ITCZ. Lake Gregory expanded during interglacial conditions over the last 400 ka and dried out during the glacial periods. In the last 1 million years, increased aridity has been linked to the expansion of dune fields in the Simpson Desert across central Australia.

5.4 Paleogene to Neogene paleomonsoon

Our synthesis of the history of the *Australian Monsoon* (*sensu stricto*), *Quasi-* and *Pseudo-Monsoon* regions has mainly focused on middle to late Pleistocene records as records of these times are best preserved in offshore and onshore Australia and therefore most researched. Deeper time records have been cored by ODP Leg 133 (Feary et al. 1993; Exon et al. 1992) and IODP Legs 356 and 363 (Gallagher et al. 2017; Rosenthal et al. 2018) around northern Australia. We describe the *Pseudo-Monsoon* record off West Australia at ODP Sites 762 and 763 and IODP Site U1463 and U1464.

Results from IODP Expedition 356 Sites U1463 and U1464 (Loc. 27, Table 1, Figs. 1, 11) showed that natural gamma radiation spectra of %K, Th ppm and U ppm represent proxies for fluvial and eolian influx tracking the

transition between arid and humid climates over the last 18 Ma (Christensen et al. 2017; Groeneveld et al. 2017). Elemental records from Sites U1463 and U1464 in combination with the recovery of sabkha-like sediments at IODP Site U1464 showed that northwest Australia was very arid throughout the year from the middle to the late Miocene (Groeneveld et al. 2017; Petrick et al. 2019). Near the Miocene-Pliocene transition, a rapid shift in the elemental records, supported by a change in sedimentation, indicates an abrupt transition to much wetter conditions, defined as the Humid Interval at ~5.5 Ma (Fig. 11; Christensen et al. 2017; Groeneveld et al. 2017; Karatsolis et al. 2020). The deposition of the massive, siliciclastic Bare Formation on the northwest shelf illustrates the change to increased river input related to wetter climate (Tagliaro et al. 2021). As U, as indicator for dust, is nearly absent from the elemental records, rainfall was probably year-round until ~3.3 Ma, after which it became more seasonal based on an increase in dust supply (Christensen et al. 2017). The northward movement of Australia led to gradual ITF constriction (Karas et al. 2009; Gallagher et al. 2024), decreasing continental humidity, culminating in the Arid Interval at ~2.4 Ma, (Christensen et al. 2017) when seasonal (monsoonal) and orbitally controlled precipitation became fully established. At ODP Site 762 (Loc. 28, Figs. 1, 11), XRF log(Fe/Ca) data suggest increasing precipitation from 5 to ~3.6 Ma followed by a distinct step to more arid conditions and rainfall variability after 3.5 Ma (Stuut et al. 2019; Auer et al. 2020). This is followed by an increase in the magnitude of precipitation variability (dry arid conditions alternating with monsoonal precipitation) corresponding to the onset of middle Pleistocene high-amplitude glacial cycles from 1.1 to 0.8 Ma (Lisiecki and Raymo 2005).

The “step” at ~3.5 Ma is associated with a marked increase in C₄ plants (Andrea et al. 2018) at ODP Site 763 (Loc. 33, Figs. 1, 11), which these authors suggest was caused by the onset of the Australian summer monsoon when global cooling due to Northern Hemisphere ice sheet expansion “forced” the southward migration of the ITCZ across northwestern Australia (cf. Broccoli et al. 2006) for the first time in the Cenozoic (Karatsolis et al. 2020). This was associated with strong seasonal precipitation variability and possible higher fire incidence as inferred from the relative abundance of fire-derived polycyclic aromatic hydrocarbons in the sediments at ODP Site 763 (Andrae et al. 2018; Karp et al. 2021).

Macroflora are critical for determining past continental conditions. Here, we dedicate a section to the discussion of the macrofloral records and highlight how the interpretations differ from other proxies.

Herold et al. (2011) modeled the climate of northern and interior Australia during the Miocene and compared

their results to fossil macrofloral assemblage interpretations. These authors concluded that a monsoonal precipitation regime wetter than today persisted during the middle to late Miocene, with the monsoonal front close to the present shear line in northern Australia (Figs. 1c, 3d). Older Paleogene paleontological sites in northern and central Australia are rare. The limited floral record at these sites suggests that Australia's monsoonal climate possibly initiated from the late Eocene to early Oligocene (Pole and Bowman 1996; Greenwood 1996; Bowman et al. 2010). However, these floral records are sparse and their age is often equivocal or has since been revised (Carpenter et al. 2011). For example, the Eocene to Oligocene age of the Stuart Creek silcrete macroflora (~29.5°S just south of Lake Eyre, Fig. 1) described by Greenwood (1996) has recently been revised and assigned a late Miocene to early Pliocene age (Callen 2020). This flora generally lacks fossil monsoonal genera (Carpenter et al. 2011), although it includes *Brachychiton* a possible monsoonal taxon (Greenwood 1996, Pole 1998). Other floral assemblages include the silcrete fossils at Lightning Ridge (~29.5°S near the Queensland/New South Wales border, Fig. 1). This latest Oligocene to middle Miocene or younger flora yields Fabaceae and *Brachychiton*-like leaves which might suggest a monsoonal influence (Carpenter et al. 2011). The possible monsoonal floras at Stuart Creek and Lightning Ridge which lay between 30 and 33°S paleolatitude (van Hinsbergen et al. 2015) may define the southerly limit of the Miocene monsoonal zone as modeled by Herold et al. (2011) and as suggested by Carpenter et al. (2011).

Many of the “Paleogene” floral assemblages in central and northern Australian are preserved in silcretes that are difficult to date (Taylor and Eggleton 2017) or likely Neogene. Therefore, any interpretations of such floras in terms of the evolution of the paleomonsoon must be made with caution. In addition, Eocene climate modeling suggests that Australia was too far south to be influenced by the ITCZ when the Australian paleomonsoon was a substantially “different dynamical feature and consequently the modern monsoon is a poor analogy in this region” (Huber and Golding 2012).

6 The future potential of Australian paleomonsoon archives

Our synthesis of Australian paleomonsoon history reveals that there has been significant progress in the understanding of the timing and dynamics of the paleomonsoon over the last two decades in terrestrial (palynoflora, lake shoreline, river sediments and speleothems) and marine (sediment) paleoarchives (especially in the interval covering the last 150 ka, Figs. 4 to 10).

Our review shows “older” Pleistocene records (> 300 ka, Fig. 10) with suitable proxy evidence identification and distinction between the *Australian Monsoon* (sensu stricto), *Pseudo-Monsoon* and *Quasi-Monsoon* are typically absent in continental Australia. We suggest that this absence is a preservation bias due to the generally harsh arid conditions that have intensified over the last 1 Ma in northern and central Australia (Fig. 10; Hesse et al. 2004; Martin 2006; Fujioka and Chappell 2010; Fitzsimmons et al. 2013; McLaren et al. 2014; Gallagher et al. 2014). These climatic conditions have likely destroyed much of the monsoonal evidence in these records, limiting possibilities for future research.

However, there are numerous offshore sediment archives all-around Australia that show potential to reveal the spatiotemporal dynamics of *Australian Monsoon* (sensu stricto), *Pseudo-Monsoon* and *Quasi-Monsoon* (Fig. 1b). Some of these records extend to the late Miocene (see reviews ODP and IODP *Pseudo-Monsoon* archives in Sect. 5.4, Fig. 11), and can be complemented by industrial wireline natural gamma radiation data from petroleum wells that provide wider regional coverage, albeit with more limited data types.

Preliminary palynofloral analyses of the 2 Ma *Quasi-Monsoon* record at ODP Site 820 (Fig. 10; Kershaw et al. 2003) from ODP Leg 133 (McKenzie and Davies 1993 and summarized in Davies 2011) on Australia's northeast margin reveal a varying rainforest flora likely related to the relative monsoonal intensity. Future palynofloral analyses of this section at higher resolution with geochemical analyses (e.g., XRF core scanning) will likely reveal the glacial/interglacial dynamics of the *Quasi-Monsoon* across the Mid Pleistocene transition from 1.1 to 0.8 Ma. In addition, there are several other fully cored sections drilled by ODP Leg 133 off northeast Australia that extend the potential monsoon record to the latest Miocene (McKenzie and Davies 1993; Davies 2011). Further analyses of these sections using various proxies are recommended to investigate when “modern” *Quasi-Monsoon* dynamics were established and if it indeed initiated in the middle Pliocene due to the synchronous southern migration of the ITCZ, as suggested for the *Pseudo-Monsoon* off northwest Australia (see Sect. 5).

Future studies might also focus on more tightly connecting the pioneering and foundational work on the continental record with the offshore results. For example, Herold et al. (2011) modeled the dynamics of the Miocene climate of Australia to suggest monsoonal conditions may have been established in northernmost Australia by the latest Miocene using limited continental macrofloral records to ground truth their model. There is an opportunity in the future to provide more detailed climate ground truthing into this modeling using

interpretations of Neogene IODP/ODP climate records cored off northwest and northeast Australia. We suggest similar regional modeling might be extended to the Pliocene Australian paleomonsoon as part of the global Pliocene Research, Interpretation and Synoptic Mapping (PRISM) marine paleoclimate reconstruction (Dowsett, et al. 2013; McClymont et al. 2020).

7 Summary of Australian Cenozoic monsoonal history

The modern Australian monsoon is a dynamic seasonal feature that is primarily controlled by the location of the ITCZ and the position of the monsoonal shear zone (Figs. 1, 2). The monsoon causes significant precipitation in the austral summer alternating with dry winter conditions across northern Australia and infills large ephemeral lakes in central Australia (Fig. 1c, d). Atmospheric circulation patterns are used to classify the Australian monsoon into a northwestern **Pseudo-Monsoon**, a northeastern **Quasi-Monsoon**, and an **Australian Monsoon** (*sensu stricto*) north of Australia (Fig. 1).

Analyses of terrestrial and marine archives from these three monsoonal regions across northern and central Australia reveals the following history:

1. **The Paleogene monsoon:** Evidence for the existence of a Paleogene Australian paleomonsoon is equivocal. Limited floral evidence across Australia is either poorly constrained stratigraphically, poorly preserved, or hosts “possible” seasonal/monsoonal taxa of unknown affinity that have been re-dated to the Neogene. In addition, modeling suggests that Australia was too far south to be affected by the ITCZ, and seasonal precipitation was different from today.
2. **Miocene Monsoonal onset:** Modeling and tectonic evidence suggests that the northern part of the Australian Plate migrated to the (sub)tropical region (north of 30°S) creating “modern” boundary conditions for monsoonal onset by the late Miocene ~10 Ma (see Fig. 3d). This is possibly supported by the presence of recently identified “monsoonal” flora in central Australia. Neogene evidence of the Australian paleomonsoon is sparse especially in terrestrial archives. There are potential archives of the *Quasi-Monsoon* in ODP cores off Queensland. However, these require additional research to investigate the Neogene history of this monsoon to determine the onset timing and dynamics of this monsoonal system. Various IODP and ODP cores off northwest Australia reveal the long-term (Neogene) climate history of the *Pseudo-Monsoon*. Arid late Miocene and warm, humid Pliocene conditions off northwest Australia were followed by *Pseudo-Monsoon* initiation at ~3.5 Ma when northern hemisphere glacial expansion “forced” the ITCZ southward across the region for the first time.
3. **Monsoonal evolution from the Pliocene to the middle Pleistocene transition:** After 3.5 Ma, marked variability in rainfall events and arid periods typified the switch to Quaternary high-amplitude glacio-eustatic cycles. This persisted to ~1 Ma when the continental climate transitioned to more arid conditions associated with the expansion of deserts in central Australia.
4. **Pseudo-Monsoon history from 1 Ma to 25 ka:** The best records of this time interval are from northwest Australia where Quaternary *Pseudo-Monsoon* marine shelfal archives reveal alternations of monsoonal siliciclastic input during wetter interglacials that alternate with drier (glacial) conditions and carbonate deposition. This suggests that glacial/interglacial cyclicity modulated monsoonal intensity when the ITCZ migrated northward during glacial and southward during interglacial periods. Monsoonal precipitation increased markedly during glacial terminations from ~1 Ma to the present paced by precession and obliquity with the onset of high-amplitude glacial/interglacial cycles whereas prior to ~1 Ma monsoonal rainfall intensity was paced by precessional cycles.
5. **Pleistocene history of the Australia Monsoon sensu stricto from 400 to 25 ka:** Terrestrial archives of the *Australian Monsoon* (*sensu stricto*) are confined to lakes and rivers younger than 400 ka in central and northern Australia. Mega-lake expansion and fluvial intensification generally corresponds to wetter interglacial periods. Abrupt millennial-scale events may have influenced the monsoonal shorelines of Lake Eyre in the absence of a clear insolation control. However, further analyses of similar shoreline deposits are required to confirm this. Marine archives of the *Australian Monsoon* (*sensu stricto*) at low latitudes off PNG and in the Timor Sea record show drier glacial and wetter interglacial periods over the last 150 ka, with persistent high summer rainfall suggesting these regions lay at or north of the ITCZ. Marine proxy evidence off PNG suggests a strong obliquity control on the *Australian Monsoon* over the last 280 ka.
6. **The Quasi-Monsoon record from 1 Ma to 25 ka:** Middle Pleistocene and older records of the *Quasi-Monsoon* are not well-known and may be preserved in marine archives off northeast Australia where ODP sites have cored sections beyond 2 Ma; further analyses of these records will like reveal the deep time record of this important monsoonal region.

7. **Australian Monsoon (*sensu stricto*) (25 to 0 ka):** Monsoonal conditions intensified near the base of the Holocene as the ITCZ migrated across *all* of northern Australia. Terrestrial and marine archives suggest the *Australian Monsoon* (*sensu stricto*) initiated from 12.5 to 11 ka with the flooding of Lake Eyre, intensification in the period from 9 to 2 ka followed by weakening possibly due to the onset of ENSO conditions.
8. **Quasi-Monsoon (25 to 0 ka):** Limited terrestrial records suggest a precipitation maximum from ~9 to ~2 ka suggesting the ITCZ reached as far south as 17°S by 9 ka. This was followed by drying after ~2 ka, suggesting a reduction in *Quasi-Monsoon* intensity.
9. **Pseudo-Monsoon (25 to 0 ka):** A weak *Pseudo-Monsoon* established off northwest Australia at ~14.5 ka and intensified from 11.5 to 7 ka in the Fitzroy River catchment. Further south in the De Grey and Fortescue River catchments, *Pseudo-Monsoon* intensification was diachronous ranging from 11.5 to 8 ka at Cape Range (22°S). This likely records the migration of the monsoon shear line southward reaching its present position by 8 ka, while the most southerly extension of the ITCZ was at ~20°S. The *Pseudo-Monsoon* weakened after ~7 ka north of 15°S and ~5 ka to the south.

In the absence of a topographic influence, a combination of insolation (precession/obliquity), abrupt millennial events and/or ITCZ variability across northern Australia have been important controls on Australian paleomonsoon intensity during the Quaternary. Further investigations of deeper time Neogene “legacy” ODP and more recent IODP cores will reveal the longer-term history of this important monsoonal domain.

Supplementary Information

The online version contains supplementary material available at <https://doi.org/10.1186/s40645-024-00662-7>.

Supplementary Materials: Figure S1. Palyonofloral data from various monsoonal archives around northern Australia adapted from Kershaw and van der Kaars (2006), see Table 1 for location and proxy details for each site. The wet and dry season (ETP) insolation from 0 to 20°S is shown.

Acknowledgements

We would like to thank Takuya Sagawa for inviting this submission. We thank also Takuya and Ryuji Tada and several anonymous reviewers for their comments that improved the manuscript. This paper was originally presented at the start of 2021 as part of a series of monsoonal seminars <https://www.youtube.com/watch?v=bALQnqlfc-U> via <https://www.monsoongeoseminars.com/>.

Author contributions

SG proposed the review topic. All authors collaborated with the corresponding author in the construction of manuscript. All authors read and approved the final manuscript.

Funding

Funding to SJG was provided by the Australian IODP office.

Availability of data and material

All data in this review MS have been plotted from previously published datasets.

Competing interests

The authors declare that they have no competing interests.

Author details

¹School of Geography, Earth and Atmospheric Sciences, University of Melbourne, Melbourne 3052, Australia. ²NAWI Graz Geocenter, Institute of Earth Sciences, University of Graz, Heinrichstrasse 26, 8010 Graz, Austria. ³Institute of Geology and Paleontology, University of Münster, Corrensstr 24, 48149 Münster, Germany. ⁴Institute of Oceanography, National Taiwan University, No. 1, Section 4, Roosevelt Road, Da’an District, 10617 Taipei, Taiwan (R.O.C.). ⁵Department of Environmental Science, Rowan University, 201 Mullica Hill Road, Glassboro, NJ 08028, USA.

Received: 12 June 2023 Accepted: 28 October 2024

Published online: 21 November 2024

References

- An Z (2000) The history and variability of the east Asian paleomonsoon climate. *Quatern Sci Rev* 19(1–5):171–187. [https://doi.org/10.1016/S0277-3791\(99\)00060-8](https://doi.org/10.1016/S0277-3791(99)00060-8)
- Andrae JW, McInerney FA, Polissar PJ, Sniderman JMK, Howard S, Hall PA, Phelps SR (2018) Initial expansion of C4 vegetation in Australia during the late Pliocene. *Geophys Res Lett* 45(10):4831–4840. <https://doi.org/10.1029/2018GL077833>
- Arkin P, Xie P (Eds) (2022) The climate data guide: CMAP: CPC merged analysis of precipitation. <https://climatedataguide.ucar.edu/climate-data/cmap-cpc-merged-analysis-precipitation>. Accessed 30 May 2022
- Auer G, Hauzenberger CA, Reuter M, Piller WE (2016) Orbitally paced phosphogenesis in Mediterranean shallow marine carbonates during the middle Miocene M onterey event. *Geochem Geophys Geosyst* 17(4):1492–1510
- Auer G, Petrick B, Yoshimura T, Mamo BL, Reuning L, Takayanagi H, De Vleeschouwer D, Martinez-Garcia A (2021) Intensified organic carbon burial on the Australian shelf after the Middle Pleistocene transition. *Quatern Sci Rev* 262:106965
- Auer G, De Vleeschouwer D, Smith R, Bogus KA, Groeneveld J, Grunert P, Castañeda I, Patrick B, Christensen BA, Fulthorpe CS, Gallagher SJ, Henderiks J (2019) Timing and pacing of Indonesian throughflow restriction to late Pliocene climate shifts. *Paleoceanogr Paleoclimatol* 34(4):635–657. <https://doi.org/10.1029/2018PA003512>
- Auer G, De Vleeschouwer D, Christensen BA (2020) Toward a robust Pliocene chronostratigraphy for ODP Site 762. *Geophys Res Lett* 47(3):2019GL085198
- Baczynski AA, McInerney FA, Freeman KH, Wing SL (2019) Carbon isotope record of trace n-alkanes in a continental PETM section recovered by the Bighorn basin coring project (BBCP). *Paleoceanogr Paleoclimatol* 34(5):853–865
- Baker PA (2009) Paleo-precipitation indicators. *Encycl Earth Sci Ser Encycl Paleoclimatol Anc Environ* 47:746–748
- Beaufort L, Kaars S, Bassinot FC, Moron V (2010) Past dynamics of the Australian monsoon: precession, phase and links to the global monsoon concept. *Clim past* 6(5):695–706
- Birks HJB, Seppä HEIKKI (2004) Pollen-based reconstructions of late-Quaternary climate in Europe—progress, problems, and pitfalls. *Acta Palaeobot* 44(2):317–334
- Blewett R (2012) *Shaping a nation: a geology of Australia*. ANU Press, Acton, ACT
- Bowler JM, Wyrwoll KH, Lu Y (2001) Variations of the northwest Australian summer monsoon over the last 300,000 years: the paleohydrological record of the gregory (Mulan) lakes system. *Quatern Int* 83:63–80

- Bowman DM, Brown GK, Braby MF, Brown JR, Cook LG, Crisp MD, Ford F, Bowman DM, Brown GK, Braby MF, Brown JR, Cook LG, Crisp MD, Ford F, Haberle S, Hughes J, Isagi Y, Joseph L (2010) Biogeography of the Australian monsoon tropics. *J Biogeogr* 37(2):201–216
- Broccoli AJ, Dahl KA, Stouffer RJ (2006) Response of the ITCZ to Northern hemisphere cooling. *Geophys Res Lett*. <https://doi.org/10.1029/2005GL024546>
- Burrows MA, Heijnis H, Gadd P, Haberle SG (2016) A new late quaternary palaeohydrological record from the humid tropics of northeastern Australia. *Palaeogeogr Palaeoclimatol Palaeoecol* 451:164–182
- Burton KW, Vance D (2000) Glacial–interglacial variations in the neodymium isotope composition of seawater in the bay of Bengal recorded by planktonic foraminifera. *Earth Planet Sci Lett* 176(3–4):425–441
- Callen RA (2020) Neogene Billa Kalina basin and Stuart Creek silicified floras, northern South Australia: a reassessment of their stratigraphy, age and environments. *Aust J Earth Sci* 67(5):605–626
- Carpenter RJ, Goodwin MP, Hill RS, Kanold K (2011) Silcrete plant fossils from lightning ridge, New South Wales: new evidence for climate change and monsoon elements in the Australian Cenozoic. *Aust J Bot* 59(5):399–425
- Christensen BA, Renema W, Henderiks J, De Vleeschouwer D, Groeneveld J, Castañeda I, Reuning L, Bogus KA, Auer G, Ishiwa T, McHugh CM, Gallagher SJ, Fulthorpe CS (2017) Indonesian throughflow drove Australian climate from humid Pliocene to arid Pleistocene. *Geophys Res Lett* 44:2977. <https://doi.org/10.1002/2017GL072977>
- Clift P, Betzler C, Clemens S, Christensen B, Eberli G, France-Lanord C, Gallagher SJ, Holbourn A, Kuhnt W, Murray R, Rosenthal Y (2022) A synthesis of monsoon exploration in the Asian marginal seas. *Sci Drill* 10:1–29. <https://doi.org/10.5194/sd-10-1-2022>
- Cohen TJ, Nanson GC, Jansen JD, Jones BG, Jacobs Z, Larsen JR, May JH, Treble P, Price DM, Smith AM (2012) Late QUATERNARY mega-lakes fed by the northern and southern river systems of central Australia: varying moisture sources and increased continental aridity. *Palaeogeogr Palaeoclimatol Palaeoecol* 356:89–108
- Cohen TJ, Jansen JD, Gliganic LA, Larsen JR, Nanson GC, May JH, Jones BG, Price DM (2015) Hydrological transformation coincided with megafaunal extinction in central Australia. *Geology* 43(3):195–198
- Davies PJ (2011) Great Barrier Reef: origin, evolution, and modern development. *Encyclopedia of modern coral reefs*. Springer, Cham, pp 504–534
- De Deckker P (2019) An evaluation of Australia as a major source of dust. *Earth Sci Rev* 194:536–567
- De Deckker P, Barrows TT, Rogers J (2014) Land–sea correlations in the Australian region: post-glacial onset of the monsoon in northwestern Western Australia. *Quatern Sci Rev* 105:181–194
- De Vleeschouwer D, Dunlea AG, Auer G, Anderson CH, Brumsack H, de Loach A, Gurnis MC, Huh Y, Ishiwa T, Jang K, Kominz MA, Marz C, Schnetger B, Murray RW, Palike H (2017) Quantifying K, U, and Th contents of marine sediments using shipboard natural gamma radiation measured on DV JOIDES resolution. *Geochem Geophys Geosyst* 18:1053–1064. <https://doi.org/10.1002/2016GC006715>
- De Vleeschouwer D, Auer G, Smith R, Bogus K, Christensen B, Groeneveld J, Petrick B, Henderiks J, Castañeda IS, O'Brien E, Ellinghausen M (2018) The amplifying effect of Indonesian throughflow heat transport on late Pliocene Southern hemisphere climate cooling. *Earth Planet Sci Lett* 500:15–27
- De Vleeschouwer D, Petrick BF, Martinez-Garcia A (2019) Stepwise weakening of the Pliocene Leeuwin current. *Geophys Res Lett* 46(14):8310–8319
- De Vleeschouwer D, Peral M, Marchegiano M, Füllberg A, Meinicke N, Pälke H, Auer G, Petrick B, Snoeck C, Goderis S, Claeys P (2022) Plio-Pleistocene Perth basin water temperatures and Leeuwin current dynamics (Indian Ocean) derived from oxygen and clumped-isotope paleothermometry. *Clim Past* 18(5):1231–1253
- Denniston RF, Wyrwoll KH, Polyak VJ, Brown JR, Asmerom Y, Wanamaker AD Jr, LaPointe Z, Ellerbroek R, Barthelmes M, Cleary D, Cugley J (2013a) A Stalagmite record of Holocene Indonesian–Australian summer monsoon variability from the Australian tropics. *Quatern Sci Rev* 78:155–168
- Denniston RF, Wyrwoll KH, Asmerom Y, Polyak VJ, Humphreys WF, Cugley J, Woods D, LaPointe Z, Peota J, Greaves E (2013b) North Atlantic forcing of millennial-scale Indo–Australian monsoon dynamics during the last glacial period. *Quatern Sci Rev* 72:159–168
- Denniston RF, Asmerom Y, Polyak VJ, Wanamaker AD Jr, Ummenhofer CC, Humphreys WF, Cugley J, Woods D, Lucker S (2017) Decoupling of monsoon activity across the northern and southern Indo-Pacific during the late glacial. *Quatern Sci Rev* 176:101–105
- Dodson JR, Macphail MK (2004) Palynological evidence for aridity events and vegetation change during the middle Pliocene, a warm period in Southwestern Australia. *Global Planet Change* 41(3–4):285–307
- Donders TH, Haberle SG, Hope G, Wagner F, Visscher H (2007) Pollen evidence for the transition of the Eastern Australian climate system from the post-glacial to the present-day ENSO mode. *Quatern Sci Rev* 26(11–12):1621–1637
- Dowsett HJ, Robinson MM, Stoll DK, Foley KM, Johnson AL, Williams M, Riesselman CR (2013) The PRISM (Pliocene palaeoclimate) reconstruction: time for a paradigm shift. *Philos Trans R Soc Math Phys Eng Sci* 371(2011):20120524
- Duller GA (2004) Luminescence dating of quaternary sediments: recent advances. *J Quatern Sci* 19(2):183–192
- Eglinton G, Logan GA (1991) Molecular preservation. *Philos Trans R Soc Lond Ser B Biol Sci* 333(1268):315–328
- Ehleringer JR, Monson RK (1993) Evolutionary and ecological aspects of photosynthetic pathway variation. *Annu Rev Ecol Syst* 24(1):411–439
- EPICA Community Members (2006) One-to-one coupling of glacial climate variability in Greenland and Antarctica. *Nature* 444:195–198
- Exon NF, Haq BU, Von Rad U (1992) Exmouth Plateau revisited: scientific drilling and geological framework. *Proc Ocean Drill Program Sci Results* 122:3–20
- Exon N, Kennett J, Malone M, Nürnberg D (2000) The opening of the Tasmanian gateway drove global Cenozoic paleoclimatic and paleoceanographic changes: results of Leg 189. *Joides J* 26(2):11–18
- Fagel N (2007) Chapter four clay minerals, deep circulation and climate. *Dev Mar Geol* 1:139–184
- Fairchild IJ, Treble PC (2009) Trace elements in speleothems as recorders of environmental change. *Quatern Sci Rev* 28(5–6):449–468
- Feary DA, Symonds PA, Davies PJ, Pigram CJ, Jarrard RD, McKenzie JA, Palmer-Julson A (1993) Geometry of Pleistocene facies on the great barrier reef outer shelf and upper slope—seismic stratigraphy of sites 819, 820, and 821. *Proc Ocean Drill Program Sci Results* 133:327–351
- Field E, McGowan HA, Moss PT, Marx SK (2017) A late Quaternary record of monsoon variability in the northwest Kimberley, Australia. *Quatern Int* 449:119–135
- Field E, Tyler J, Gadd PS, Moss P, McGowan H, Marx S (2018) Coherent patterns of environmental change at multiple organic spring sites in northwest Australia: evidence of Indonesian–Australian summer monsoon variability over the last 14,500 years. *Quatern Sci Rev* 196:193–216
- Fitzsimmons KE, Miller GH, Spooner NA, Magee JW (2012) Aridity in the monsoon zone as indicated by desert dune formation in the Gregory Lakes basin, northwestern Australia. *Aust J Earth Sci* 59(4):469–478
- Fitzsimmons KE, Cohen TJ, Hesse PP, Jansen J, Nanson GC, May JH, Barrows TT, Haberlah D, Hilgers A, Kelly T, Larsen J (2013) Late Quaternary palaeoenvironmental change in the Australian drylands. *Quatern Sci Rev* 74:78–96
- Fu X, Cohen TJ, Arnold LJ (2017) Extending the record of lacustrine phases beyond the last interglacial for Lake Eyre in central Australia using luminescence dating. *Quatern Sci Rev* 162:88–110
- Fujioka T, Chappell J (2010) History of Australian aridity: chronology in the evolution of landscapes. *Geol Soc Spec Pub* 346(1):121–139. <https://doi.org/10.1144/SP346.829>
- Fujioka T, Chappell J, Fifield LK, Rhodes EJ (2009) Australian desert dune fields initiated with Pliocene–Pleistocene global climatic shift. *Geology* 37(1):51–54
- Gallagher SJ, deMenocal PB (2019) Finding dry spells in Ocean sediments. *Oceanography* 32(1):38–41. <https://doi.org/10.5670/oceanog.2019.120>
- Gallagher SJ, Wagstaff BE (2021) Quaternary environments and monsoonal climate off northwest Australia: palynological evidence from Ocean drilling program site 765. *Quatern Sci Rev* 259:106917
- Gallagher SJ, Wallace MW, Hoiles PW, Southwood JM (2014) Seismic and stratigraphic evidence for reef expansion and onset of aridity on the Northwest Shelf of Australia during the Pleistocene. *Mar Pet Geol* 57:470–481. <https://doi.org/10.1016/j.marpetgeo.2014.06.011>
- Gallagher SJ, Fulthorpe CS, Bogus KA (2017) Expedition 356 Summary. *Proc IODP* 356:1–43. <https://doi.org/10.14379/iodp.proc.356.101.2017>

- Gallagher SJ, Reuning L, Himmler T, Henderiks J, De Vleeschouwer D, Groenewald J, Rastiger A, Fulthorpe CS, Bogus K (2018) The enigma of rare quaternary Oolites in the Indian and Pacific Oceans: a result of global oceanographic physicochemical conditions or a sampling bias. *Quatern Sci Rev* 200:114–122. <https://doi.org/10.1016/j.quascirev.2018.09.028>
- Gallagher SJ, Auer G, Brierley C, Fulthorpe CS, Hall R (2024) Cenozoic history of the Indonesian gateway. *Ann Rev Earth Planet Sci* 52:106302. <https://doi.org/10.1146/annurev-earth-040722-111322>
- Gentili J (1971) *Climates of Australia and New Zealand*. Elsevier Pub. Co., Amsterdam
- Gentili J (1995) Holocene climates of the Northern Australian region. *J Coastal Res* 17:119–121
- Geoscience Australia (2015) Radmap unfiltered ppm Uranium v3. [Available at <http://www.ga.gov.au/>. Commonwealth of Australia.]
- Gingele FX, De Deckker P, Hillenbrand CD (2001) Clay mineral distribution in surface sediments between Indonesia and NW Australia—source and transport by ocean currents. *Marine Geol* 179(3–4):135–146
- Gong L, Holbourn A, Kuhnt W, Opdyke B, Zhang Y, Ravelo AC, Zhang P, Xu J, Matsuzaki K, Aiello I, Beil S (2023) Middle Pleistocene re-organization of Australian Monsoon. *Nat Commun* 14(1):2002
- Griffiths ML, Drysdale RN, Gagan MK, Zhao JX, Ayliffe LK, Hellstrom JC, Hantoro WS, Frisia S, Feng YX, Cartwright I, Pierre ES (2009) Increasing Australian-Indonesian monsoon rainfall linked to early Holocene sea-level rise. *Nat Geosci* 2(9):636–639
- Griffiths ML, Drysdale RN, Gagan MK, Frisia S, Zhao JX, Ayliffe LK, Hantoro WS, Hellstrom JC, Fischer MJ, Feng YX, Suwargadi BW (2010) Evidence for Holocene changes in Australian-Indonesian monsoon rainfall from stalagmite trace element and stable isotope ratios. *Earth Planet Sci Lett* 292(1–2):27–38
- Groenewald J, Henderiks J, Renema W, McHugh CM, De Vleeschouwer D, Christensen BA, Fulthorpe CS, Reuning L, Gallagher SJ, Bogus KA, Auer G, Ishiwa T (2017) Australian shelf sediments reveal shifts in Miocene southern Hemisphere Westerlies. *Sci Adv* 3:e1602567
- Groenewald J, De Vleeschouwer D, McCaffrey J, Gallagher SJ (2021) Dating the northwest shelf of Australia since the Pliocene. *Geochem Geophys Geosyst* 22:2020GC009418. <https://doi.org/10.1029/2020GC009418>
- Gurnis M, Kominz M, Gallagher SJ (2020) Reversible subsidence on the North West Shelf of Australia. *Earth Planet Sci Lett* 534:116070. <https://doi.org/10.1016/j.epsl.2020.116070>
- Haberle SG (2005) A 23,000-yr pollen record from Lake Euramoo, wet tropics of NE Queensland Australia. *Quatern Res* 64(3):343–356
- Hallenberger M, Reuning L, Gallagher SJ, Back S, Ishiwa T, Christensen BA, Bogus K (2019) Increased fluvial runoff terminated inorganic aragonite precipitation on the Northwest Shelf of Australia during the early Holocene. *Sci Rep* 9:18356. <https://doi.org/10.1038/s41598-019-54981-7>
- Harris AJ, Papes M, Gao YD, Watson L (2014) Estimating paleoenvironments using ecological niche models of nearest living relatives: A case study of Eocene *Aesculus* L. *J Syst Evol* 52(1):16–34
- Herold N, Huber M, Greenwood DR, Müller RD, Seton M (2011) Early to middle Miocene monsoon climate in Australia. *Geology* 39(1):3–6
- Hesse PP (2016) How do longitudinal dunes respond to climate forcing? Insights from 25 years of luminescence dating of the Australian desert dunefields. *Quatern Int* 410:11–29
- Hesse PP, McTainsh GH (2003) Australian dust deposits: modern processes and the quaternary record. *Quatern Sci Rev* 22(18–19):2007–2035
- Hesse PP, Magee JW, van der Kaars S (2004) Late quaternary climates of the Australian arid zone: a review. *Quatern Int* 118:87–102
- Hesselbo SP (1996) Spectral Gamma-ray logs in relation to clay mineralogy and sequence stratigraphy, Cenozoic of the Atlantic margin, offshore New Jersey 1. In: *Proceedings of the ocean drilling program: scientific results*, vol 150, pp 411
- Hladil J, Gersl M, Strnad L, Frana J, Langrova A, Spisiak J (2006) Stratigraphic variation of complex impurities in platform limestones and possible significance of atmospheric dust: a study with emphasis on gamma-ray spectrometry and magnetic susceptibility outcrop logging (Eifelian-Frasnian, Moravia, Czech Republic). *Int J Earth Sci* 95(4):703–723
- Hobbs JE, Lindesay J, Bridgman HA (eds) (1998) *Climates of the southern continents: present, past and future*, vol 297. Wiley, New York, USA
- Holbourn A, Kuhnt W, Kawamura H, Jian Z, Grootes P, Erlenkeuser H, Xu J (2005) Orbitally paced paleoproductivity variations in the Timor Sea and Indonesian throughflow variability during the last 460 kyr. *Paleoceanography*. <https://doi.org/10.1029/2004PA001094>
- Hollis CJ, Dunkley Jones T, Anagnostou E, Bijl PK, Cramwinckel MJ, Cui Y, Dickens GR, Edgar KM, Eley Y, Evans D, Foster GL (2019) The DeepMIP contribution to PMIP4: methodologies for selection, compilation and analysis of latest Paleocene and early Eocene climate proxy data, incorporating version 0.1 of the DeepMIP database. *Geosci Model Dev* 12(7):3149–3206
- Huber M, Goldner A (2012) Eocene Monsoons. *J Asian Earth Sci* 44:3–23
- Isdale P (1984) Fluorescent bands in massive corals record centuries of coastal rainfall. *Nature* 310(5978):578–579
- Ishiwa T, Yokoyama Y, Reuning L, McHugh CM, De Vleeschouwer D, Gallagher SJ (2019) Australian summer monsoon variability in the past 14,000 years revealed by IODP expedition 356 sediments. *Prog Earth Planet Sci* 6:1–17. <https://doi.org/10.1186/s40645-019-0262-5>
- Karas C, Nürnberg D, Gupta AK, Tiedemann R, Mohan K, Bickert T (2009) Mid-Pliocene climate change amplified by a switch in Indonesian subsurface throughflow. *Nat Geosci* 2(6):434–438. <https://doi.org/10.1038/ngeo520>
- Karas C, Nürnberg D, Tiedemann R, Garbe-Schönberg D (2011) Pliocene Indonesian throughflow and Leeuwin current dynamics: implications for Indian Ocean polar heat flux. *Paleoceanography* 26(2):PA2217. <https://doi.org/10.1029/2010PA001949>
- Karatsolis BT, De Vleeschouwer D, Groenewald J, Christensen B, Henderiks J (2020) The late Miocene to early Pliocene “humid interval” on the NW Australian shelf: disentangling climate forcing from regional basin evolution. *Paleoceanogr Paleoclimatol* 35(9):2019003780
- Karp AT, Andrae JW, McInerney FA, Polissar PJ, Freeman KH (2021) Soil carbon loss and weak fire feedbacks during Pliocene C4 grassland expansion in Australia. *Geophys Res Lett* 48(2):e2020GL090964
- Kawamura H, Holbourn A, Kuhnt W (2006) Climate variability and land–ocean interactions in the Indo Pacific Warm Pool: a 460-ka palynological and organic geochemical record from the Timor Sea. *Mar Micropaleontol* 59(1):1–14. <https://doi.org/10.1016/j.marmicro.2005.09.001>
- Kershaw P, Van Der Kaars S (2006) Pollen records, late pleistocene] Australia and New Zealand. *Encyclopedia of quaternary science*. Elsevier, Amsterdam, pp 2613–2623
- Kershaw P, van der Kaars S (2012) Australia and the southwest Pacific. *Quaternary environmental change in the tropics*. Wiley, New York, pp 236–262
- Kershaw AP, van der Kaars S, Moss PT (2003) Late quaternary millankovitch-scale climatic change and variability and its impact on monsoonal Australasia. *Mar Geol* 201(1–3):81–95. [https://doi.org/10.1016/S0025-3227\(03\)00210-X](https://doi.org/10.1016/S0025-3227(03)00210-X)
- Kershaw AP, Bretherton SC, van der Kaars S (2007) A complete pollen record of the last 230 ka from Lynch’s Crater, north-eastern Australia. *Palaeogeogr Palaeoclimatol Palaeoecol* 251(1):23–45
- Kock S, Kramers JD, Preusser F, Wetzel A (2009) Dating of late Pleistocene terrace deposits of the River Rhine using Uranium series and luminescence methods: potential and limitations. *Quatern Geochronol* 4(5):363–373
- Krause CE, Gagan MK, Dunbar GB, Hantoro WS, Hellstrom JC, Cheng H, Edwards RL, Suwargadi BW, Abram NJ, Rifai H (2019) Spatio-temporal evolution of Australasian monsoon hydroclimate over the last 40,000 years. *Earth Planet Sci Lett* 513:103–112
- Kuhnt W, Holbourn A, Xu J, Opdyke B, De Deckker P, Röhl U, Mudelsee M (2015) Southern hemisphere control on Australian Monsoon variability during the late deglaciation and Holocene. *Nat Commun* 6(1):1–7
- Lisiecki LE, Raymo ME (2005) A Pliocene–Pleistocene stack of 57 globally distributed benthic $\delta^{18}O$ records. *Paleoceanography* 20(1):1003. <https://doi.org/10.1029/2004PA001071>
- Liu Y, Lo L, Shi Z, Wei KY, Chou CJ, Chen YC, Chuang CK, Wu CC, Mii HS, Peng Z, Amakawa H (2015) Obliquity pacing of the western Pacific intertropical convergence zone over the past 282,000 years. *Nat Commun* 6(1):1–7
- Lough JM (2007) Tropical river flow and rainfall reconstructions from coral luminescence: great barrier reef Australia. *Paleoceanography*. <https://doi.org/10.1029/2006PA001377>
- Lough JM, Llewellyn LE, Lewis SE, Turney CS, Palmer JG, Cook CG, Hogg AG (2014) Evidence for suppressed mid-Holocene northeastern Australian monsoon variability from coral luminescence. *Paleoceanography* 29(6):581–594

- Macphail MK, Hill RS (2018) What was the vegetation in northwest Australia during the Paleogene, 66–23 million years ago? *Aust J Bot* 66(7):556–574
- Magee JW, Miller GH, Spooner NA, Questiaux D (2004) Continuous 150 ky monsoon record from Lake Eyre, Australia: insolation-forcing implications and unexpected Holocene failure. *Geology* 32(10):885–888. <https://doi.org/10.1130/G20672.1>
- Mann ME (2002) The value of multiple proxies. *Science* 297(5586):1481–1482
- Martin HA (2006) Cenozoic climatic change and the development of the arid vegetation in Australia. *J Arid Environ* 66(3):533–563
- McBride JL (1987) The Australian summer monsoon. *Monsoon Meteorol* 203(232):13
- McBride JL, Keenan TD (1982) Climatology of tropical cyclone genesis in the Australian region. *J Climatol* 2(1):13–33
- McClymont EL, Ford HL, Ho SL, Tindall JC, Haywood AM, Alonso-Garcia M, Bailey I, Berke MA, Littler K, Patterson MO, Petrick B (2020) Lessons from a high-CO₂ world: an ocean view from ~ 3 million years ago. *Clim past* 16(4):1599–1615
- McClymont EL, Ho SL, Ford HL, Bailey I, Berke MA, Bolton CT, De Schepper S, Grant GR, Groeneveld J, Inglis GN, Karas C (2023) Climate evolution through the onset and intensification of northern hemisphere glaciation. *Rev Geophys* 61:2022RG000793
- McDermott F (2004) Palaeo-climate reconstruction from stable isotope variations in speleothems: a review. *Quatern Sci Rev* 23(7–8):901–918
- McKenzie JA, Davies PJ (1993) Cenozoic evolution of carbonate platforms on the northeast Australian margin: synthesis of ODP Leg 133 drilling results. In: McKenzie JA, Davies PJ, Palmer-Julson A, Sarg JF (eds.), *Proceedings of ocean drilling program, scientific results*. Texas A. and M. University, College Station, TX, pp 133
- McLaren S, Wallace MW, Gallagher SJ, Wagstaff BE, Tosolini A-MP (2014) The development of a climate: an arid continent with wet fringes. In: Prins HHT, Gordon IJ (eds) *Invasion biology and ecosystem theory: insights from a continent in transformation*. Cambridge University Press, Cambridge, pp 256–280
- Muller J, Kylander M, Wüst RA, Weiss D, Martinez-Cortizas A, LeGrande AN, Jennerjahn T, Behling H, Anderson WT, Jacobson G (2008) Possible evidence for wet Heinrich phases in tropical NE Australia: the Lynch's crater deposit. *Quatern Sci Rev* 27(5–6):468–475
- Murphy BP, Bowman DM (2007) Seasonal water availability predicts the relative abundance of C3 and C4 grasses in Australia. *Glob Ecol Biogeogr* 16(2):160–169
- Nanson GC, Price DM, Short SA, Young RW, Jones BG (1991) Comparative uranium-thorium and thermoluminescence dating of weathered Quaternary alluvium in the tropics of northern Australia. *Quatern Res* 35(3):347–366
- Nanson GC, Price DM, Jones BG, Maroulis JC, Coleman M, Bowman H, Cohen TJ, Pietsch TJ, Larsen JR (2008) Alluvial evidence for major climate and flow regime changes during the middle and late quaternary in eastern central Australia. *Geomorphology* 101(1–2):109–129
- O'Brien CL, Foster GL, Martínez-Boti MA, Abell R, Rae JW, Pancost RD (2014) High sea surface temperatures in tropical warm pools during the Pliocene. *Nat Geosci* 7(8):606–611
- O'Dea A, Lessios HA, Coates AG, Eytan RI, Restrepo-Moreno SA, Cione AL, Collins LS, De Queiroz A, Farris DW, Norris RD, Stallard RF (2016) Formation of the Isthmus of Panama. *Sci Adv* 2(8):e1600883
- Pei R, Kuhnt W, Holbourn A, Hingst J, Koppe M, Schultz J, Kopetz P, Zhang P, Andersen N (2021) Monitoring Australian Monsoon variability over the past four glacial cycles. *Palaeogeogr Palaeoclimatol Palaeoecol* 568:110280
- Peng C, Zou C, Zhang S, Shu J, Wang C (2024) Geophysical logs as proxies for cyclostratigraphy: Sensitivity evaluation, proxy selection, and paleoclimatic interpretation. *Earth Sci Rev* 252:104735
- Petrick B, Martínez-García A, Auer G, Reuning L, Auderset A, Deik H, Takayanagi H, De Vleeschouwer D, Iryu Y, Haug GH (2019) Glacial Indonesian throughflow weakening across the mid-pleistocene climatic transition. *Sci Reports* 9(1):16995
- Pole MS, Bowman DJ (1996) Tertiary plant fossils from Australia's top end. *Aust Syst Bot* 9(2):113–126
- Pross J, Klotz S, Mosbrugger V (2000) Reconstructing palaeotemperatures for the early and middle Pleistocene using the mutual climatic range method based on plant fossils. *Quatern Sci Rev* 19(17–18):1785–1799
- Raymo ME (1994) The initiation of Northern Hemisphere glaciation. *Annu Rev Earth Planet Sci* 22:353–383
- Rhodes EJ (2011) Optically stimulated luminescence dating of sediments over the past 200,000 years. *Annu Rev Earth Planet Sci* 39:461–488
- Rosenthal Y, Holbourn AE, Kulhanek DK, Aiello IW, Babila TL, Bayon G, Beaufort L, Bova SC, Chun JH, Dang H, Drury AJ (2018) Expedition 363 summary. In: *Proceedings of the international ocean discovery program*
- Rothwell RG (2015a) Twenty years of XRF core scanning marine sediments: what do geochemical proxies tell us? *Micro-XRF studies of sediment cores*. Springer, Dordrecht, pp 25–102
- Rothwell RG (2015b) Micro-XRF studies of sediment cores: a perspective on capability and application in the environmental sciences. *Micro-XRF studies of sediment cores*. Springer, Dordrecht, pp 1–21
- Shulmeister J (1992) A Holocene pollen record from lowland tropical Australia. *Holocene* 2(2):107–116
- Shulmeister J, Lees BG (1995) Pollen evidence from tropical Australia for the onset of an ENSO-dominated climate at c. 4000 BP. *Holocene* 5(1):10–18
- Smith FA, Freeman KH (2006) Influence of physiology and climate on δD of leaf wax n-alkanes from C3 and C4 grasses. *Geochim Cosmochim Acta* 70(5):1172–1187
- Spooner MI, Barrows TT, De Deckker P, Paterne M (2005) Palaeoceanography of the Banda Sea, and late Pleistocene initiation of the northwest monsoon. *Global Planet Change* 49(1–2):28–46
- Stoll HM, Vance D, Arealos A (2007) Records of the Nd isotope composition of seawater from the Bay of Bengal: implications for the impact of Northern Hemisphere cooling on ITCZ movement. *Earth Planet Sci Lett* 255(1–2):213–228
- Sturman AP, Tapper NJ (1996) *The weather and climate of Australia and New Zealand*. Oxford University Press, Oxford, USA
- Stuut J-BW, Temmesfeld F, De Deckker P (2014) A 550 ka record of Aeolian activity near North West Cape, Australia: inferences from grain-size distributions and bulk chemistry of SE Indian Ocean deep-sea sediments. *Quatern Sci Rev* 83:83–94
- Stuut J-BW, De Deckker P, Saavedra-Pellitero M, Bassinot F, Drury AJ, Walczak MH, Nagashima K, Murayama M (2019) A 5.3-million-year history of monsoonal precipitation in Northwestern Australia. *Geophys Res Lett* 46(12):6946–6954
- Suppiah R (1992) The Australian summer monsoon: a review. *Prog Phys Geogr* 16(3):283–318
- Suppiah R (1995) The Australian summer monsoon: CSIRO9 GCM simulations for 1x CO₂ and 2x CO₂ conditions. *Global Planet Change* 11(3):95–109
- Tachikawa K, Piotrowski AM, Bayon G (2014) Neodymium associated with foraminiferal carbonate as a recorder of seawater isotopic signatures. *Quatern Sci Rev* 88:1–13
- Taylor G, Eggleton RA (2017) Silcrete: an Australian perspective. *Aust J Earth Sci* 64(8):987–1016
- Thiry M (2000) Palaeoclimatic interpretation of clay minerals in marine deposits: an outlook from the continental origin. *Earth Sci Rev* 49(1–4):201–221
- Thiry M, Milnes AR, Rayot V, Simon-Coinçon R (2006) Interpretation of palaeoweathering features and successive silicifications in the Tertiary regolith of inland Australia. *J Geol Soc* 163(4):723–736
- Thomson JR, Holden PB, Anand P, Edwards NR, Porchier CA, Harris NB (2021) Tectonic and climatic drivers of Asian Monsoon evolution. *Nat Commun* 12(1):4022
- Turney CS, Kershaw AP, Clemens SC, Branch N, Moss PT, Fifield LK (2004) Millennial and orbital variations of El Niño/Southern oscillation and high-latitude climate in the last glacial period. *Nature* 428(6980):306–310
- Uhl D, Mosbrugger V, Bruch A, Utescher T (2003) Reconstructing palaeotemperatures using leaf floras—case studies for a comparison of leaf margin analysis and the coexistence approach. *Rev Palaeobot Palynol* 126(1–2):49–64
- Utescher T, Bruch AA, Erdei B, François L, Ivanov D, Jacques FMB, Kern AK, Mosbrugger V, Spicer RA (2014) The coexistence approach—theoretical background and practical considerations of using plant fossils for climate quantification. *Palaeogeogr Palaeoclimatol Palaeoecol* 410:58–73
- van der Kaars S, De Deckker P (2002) A late Quaternary pollen record from deep-sea core Fr10/95, GC17 offshore Cape Range Peninsula, northwestern Western Australia. *Rev Palaeobot Palynol* 120(1–2):17–39
- van der Kaars S, De Deckker P, Gingele FX (2006) A 100 000-year record of annual and seasonal rainfall and temperature for northwestern

- Australia based on a pollen record obtained offshore. *J Quatern Sci Publ Quatern Res Assoc* 21(8):879–889
- van Hinsbergen DJ, De Groot LV, van Schaik SJ, Spakman W, Bijl PK, Sluijs A, Langeris CG, Brinkhuis H (2015) A paleolatitude calculator for paleoclimate studies. *PLoS ONE* 10(6):e0126946
- Wang XH, Zhang H (2017) Effects of Australian summer Monsoon on Sea surface temperature diurnal variation over the Australian North-Western Shelf. *Geophys Res Lett* 44(19):9856–9864
- Wang PX, Wang B, Cheng H, Fasullo J, Guo Z, Kiefer T, Liu Z (2017) The global Monsoon across time scales: mechanisms and outstanding issues. *Earth Sci Rev* 174:84–121
- Wei-Hong Q, Shuai-Qi T (2010) Identifying global monsoon troughs and global atmospheric centers of action on a pentad scale. *Atmos Ocean Sci Lett* 3(1):1–6
- Westerhold T, Marwan N, Drury AJ, Liebrand D, Agnini C, Anagnostou E, Barnett JS, Bohaty SM, De Vleeschouwer D, Florindo F, Frederichs T (2020) An astronomically dated record of Earth's climate and its predictability over the last 66 million years. *Science* 369(6509):1383–1387
- Williams M, Cook E, van der Kaars S, Barrows T, Shulmeister J, Kershaw P (2009) Glacial and deglacial climatic patterns in Australia and surrounding regions from 35 000 to 10 000 years ago reconstructed from terrestrial and near-shore proxy data. *Quatern Sci Rev* 28(23–24):2398–2419
- Wong CI, Breecker DO (2015) Advancements in the use of speleothems as climate archives. *Quatern Sci Rev* 127:1–18
- Wyrwoll KH, Miller GH (2001) Initiation of the Australian summer monsoon 14,000 years ago. *Quatern Int* 83:119–128
- Wyrwoll KH, Hopwood J, McKenzie NL (1992) The Holocene paleohydrology and climatic history of the northern Great Sandy Desert-Fitzroy Trough: with special reference to the history of the northwest Australian Monsoon. *Clim Change* 22(1):47–65
- Wyrwoll KH, Liu Z, Chen G, Kutzbach JE, Liu X (2007) Sensitivity of the Australian summer monsoon to tilt and precession forcing. *Quatern Sci Rev* 26(25–28):3043–3057
- Wyrwoll K-H, Hopwood JM, Chen G (2012) Orbital time-scale circulation controls of the Australian summer monsoon: a possible role for mid-latitude Southern Hemisphere forcing? *Quatern Sci Rev* 35:23–28. <https://doi.org/10.1016/j.quascirev.2012.01.003>
- Zachos JC, Dickens GR, Zeebe RE (2008) An early Cenozoic perspective on greenhouse warming and carbon-cycle dynamics. *Nature* 451(7176):279–283
- Zachos J, Pagani M, Sloan L, Thomas E, Billups K (2001) Trends, rhythms, and aberrations in global climate 65 Ma to present. *Science* 292(5517):686–693
- Zhang H, Moise A (2016) The Australian summer Monsoon in current and future climate. *The Monsoons and climate change*. Springer, Cham, pp 67–120
- Zhang P, Xu J, Holbourn A, Kuhnt W, Beil S, Li T, Xiong Z, Dang H, Yan H, Pei R, Ran Y (2020) Indo-Pacific hydroclimate in response to changes of the intertropical convergence zone: discrepancy on precession and obliquity bands over the last 410 kyr. *J Geophys Res Atmos* 125(14):e2019JD032125
- Zhisheng A, Kutzbach JE, Prell WL, Porter SC (2001) Evolution of Asian monsoons and phased uplift of the Himalaya-Tibetan plateau since Late Miocene times. *Nature* 411(6833):62–66

Publisher's Note

Springer Nature remains neutral with regard to jurisdictional claims in published maps and institutional affiliations.